Annu. Rev. Earth Planet. Sci. 2005. 33:605–43
doi: 10.1146/annurev.earth.33.092203.122658

First published online as a Review in Advance on February 7, 2005

ATMOSPHERIC MOIST CONVECTION

Bjorn Stevens
Department of Atmospheric and Oceanic Sciences, University of California, Los Angeles, California 90095; email: bstevens@atmos.ucla.edu

Key Words atmospheric boundary layers, atmospheric turbulence, clouds, multiphase flows, precipitation, buoyancy

■ **Abstract** Various forms of atmospheric moist convection are reviewed through a consideration of three prevalent regimes: stratocumulus; trade-wind; and deep, precipitating, maritime convection. These regimes are chosen because they are structural components of the general circulation of the atmosphere and because they highlight distinguishing features of this polymorphous phenomenon. In particular, the ways in which varied forms of moist convection communicate with remote parts of the flow through mechanisms other than the rearrangement of fluid parcels are emphasized. These include radiative, gravity wave, and/or microphysical (precipitation) processes. For each regime, basic aspects of its phenomenology are presented along with theoretical frameworks that have arisen to help rationalize the phenomenology. Recent developments suggest that the increased capacity for numerical simulation and increasingly refined remote sensing capabilities bodes well for major advances in the coming years.

1. INTRODUCTION

Moist (atmospheric) convection, manifest as clouds, engenders and embellishes the irreversibility of atmospheric motions. It expresses itself with a wonderfully rich phenomenology spanning a fantastic range of scales and is involved intricately in many of the central problems in meteorology and climate science. Severe weather, including hurricanes, flash-floods, electrical storms, and tornadoes, invariably involves deep, precipitating moist convection. Today's climate and its susceptibility to human perturbations are thought to depend on, in crucial yet subtle ways, the behavior of all forms of moist convection. Despite a concrete appreciation of its role in a wide variety of pressing problems, our understanding of this basic process remains amorphous, in part because unlike its dry counterpart, moist convection is not one or two but many things. Despite this remarkable complexity, one gets the impression that at least some of the mysteries of moist convection are beginning to succumb to the ever-increasing power of numerical simulation and remote sensing—an impression developed below when possible.

The main ideas presented in this review are limited to three basic forms of upright, maritime, moist convection, illustrated in the context of a thermally

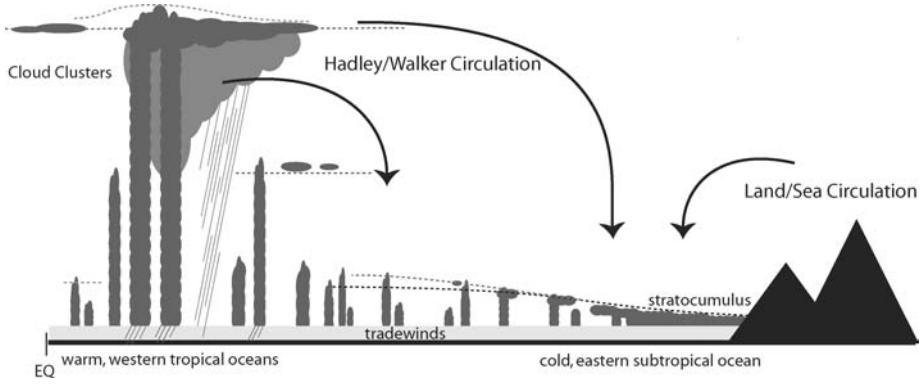

Figure 1 Cloud regimes in thermally direct circulations. Adapted from Arakawa (1975).

direct circulation in Figure 1. Here deep, ice-crowned, precipitating cumulus towers mediate rising motion near the equator; stratocumulus clouds veil the cold subtropical ocean; and in-between trade-wind cumulus deepen the atmospheric boundary layer, enhancing surface evaporation and fueling, in part, the overturning circulation. Earth's Hadley and Walker cells are often idealized in terms of such a figure, and as such the interplay between these types of moist convection and the attendent large-scale circulation is a topic of considerable interest. Even so, this is still a parochial view, both in terms of the convection itself and in terms of the large-scale circulation in which it is embedded. A full understanding of the baroclinic eddies of the midlatitudes, another engine of the general circulation, also involves an understanding of moist-convective processes, as does an understanding of orographic precipitation and atmosphere land-surface interactions. This review is also limited in that it focuses on the statistics of fields of convecting clouds, at the expense of the details of individual clouds or storm systems and their transient behavior. I also focus almost entirely on thermodynamic arguments (beginning with a review of basic concepts and terminology in Section 2), shamelessly ignoring the important question of the role of moist convection in transporting momentum (see Moncrieff 1997 for a review). Nonetheless, even such a narrow view proves adequate for organizing a great deal of recent research, and it also introduces important ways in which moist convection expresses its irreversibility—and this is key to understanding why moist convection is many things.

2. ATMOSPHERIC THERMODYNAMICS

The language of moist convection is the idiosyncratic language of moist (atmospheric) thermodynamics, where almost everything, from density, to entropy, to moisture content, finds expression as a temperature. Although elementary, and well covered in many texts (e.g., Iribarne & Godson 1973, Emanuuel 1994, Bohren & Albrecht 1998), I review the main ideas here for the benefit of those with less

background in the atmospheric sciences. For purposes of orientation, I begin by first reviewing dry atmospheric thermodynamics wherein the air is taken to be a perfect gas with a fixed composition.

2.1. Dry Air

The state of the dry system is determined by any two state variables, for instance temperature, T, and pressure, p. However, for a hydrostatic atmosphere $\partial_z p = -\rho g$ (where the density, ρ, is a function of state and g is the gravitational acceleration), the spatial distribution of T determines p as a function of the height, z. Consequently, the state of the hydrostatic system can be completely determined by the distribution of T in space and time, which we denote by (x, y, z, t) with z pointing upward. For most applications, instead of T, it proves useful to describe the state of the system in terms of the potential temperature, θ, defined as

$$\theta \equiv T \left(\frac{\pi}{p} \right)^{R/c_p}, \tag{1}$$

where π is a specified reference pressure (typically taken as 1000 hPa); $R = 287\ \mathrm{J\,kg^{-1}\,K^{-1}}$ is the gas constant; and $c_p = 1006\ \mathrm{J\,kg^{-1}\,K^{-1}}$ the isobaric specific heat of the working fluid, which in this case is "dry air," the name commonly given to an ideal mixture of N_2, O_2, and Ar (Argon) with number fractions of 0.7809, 0.2095, and 0.00934, respectively. Physically, θ is the temperature that air at some initial temperature T and pressure p would have if it were isentropically brought to a reference state pressure π; consequently, the temperature does not vary with pressure (and hence z) for isentropic displacement of fluid parcels—which is one of its chief virtues. Because entropy differences from an arbitrary reference state vary as $c_p \ln \theta$, isopleths of θ can be identified with isentropes of the system.

Vertical accelerations in the atmosphere can be associated with imbalances in gravitational and the hydrostatic component of the pressure forces, i.e., buoyancy perturbations, which appear as the first term on the right-hand side of the vertical momentum equation:

$$(\partial_t + \mathbf{u} \cdot \nabla)\, w = -g \frac{\rho'}{\rho} - \partial_z p' + \nu \nabla^2 w, \tag{2}$$

where primes denote deviations from a hydrostatic reference state, which is denoted by subscript 0 below; ν is the kinematic viscosity; and $\mathbf{u} \equiv \{u, v, w\}$ is the velocity vector. The relationship between density and the state of the system is given by the equation of state, which for a dry atmosphere is the ideal gas law, $p = \rho R T$, the linearization of which yields

$$\frac{\rho'}{\rho_0} \approx -\frac{T'}{T_0} + \frac{p'}{p_0} \approx -\frac{\theta'}{\theta_0} + \left(\frac{c_v}{c_p} \right) \frac{p'}{p_0}, \tag{3}$$

where c_v is the isometric specific heat of the working fluid. For most scales of motion in the troposphere, $\rho' \ll \rho_0$. Because it is also possible to pick a basic

state such that pressure perturbations contribute negligibly to density variations, the buoyancy can be related to the state of the system as

$$b = -g\frac{\rho'}{\rho} \approx -g\frac{\rho'}{\rho_0} \approx g\frac{\theta'}{\theta_0}. \tag{4}$$

Hence buoyancy is effectively proportional to entropy variations.

In the nondiffusive, inviscid limit, it is straightforward to show that for a horizontally homogeneous fluid at rest, at any given point the fluid is stable, neutral, or unstable to infinitesimal perturbations according to whether $\partial_z\theta$ is greater than, equal to, or less than zero, respectively. In response to such an instability, the fluid convects with the purpose of rearranging fluid parcels so that θ is nondecreasing. In practice, these motions induce filamentation of fluid elements, which then lays the basis for molecular dissipation of temperature (buoyancy) and velocity perturbations; thus convection tends to drive the fluid to the neutrally stratified state of $\partial_z\theta = 0$, which under suitably chosen constraints is also the state of maximum entropy (Verkley & Gerkema 2004). In such a state, $\Gamma_d \equiv \partial_z T = -g/c_p$, which is exactly the lapse rate in temperature required so that the reduction in the specific enthalpy (c_pT) with height equals the increase in the potential energy (gz). This is called the dry-adiabatic lapse rate and is precisely what is to be expected for isentropic, vertical displacements of dry fluid parcels.

2.2. Moist (Warm) Air

To describe the state of a moist atmosphere requires some measure of the water within a control volume. A common choice is q_t, the total water specific humidity (defined as the mass fraction of H_2O in the system). The mass fraction of dry air follows as the remainder, $q_d = 1 - q_t$. Although the partitioning of water mass among its vapor q_v, and condensate q_c forms (which can be liquid, denoted q_l, or ice, denoted q_i) is a strong function of temperature (and hence pressure, and equivalently altitude), q_t does not change following reversible fluid displacements. The presence of a variable constituent in the moist system implies that partial derivatives of the working fluid (the gas constant, specific heats, etc.) will vary with the composition of the fluid. Both this and phase changes complicate the development of the thermodynamics of moist air. Because the propensity of ice toward nonequilibrium introduces particular complications and because many of the interesting aspects of moist convecting atmospheres are apparent in the absence of ice, most of our ensuing development is for convection in the absence of ice processes.

Similar to the dry system, instead of temperature, it is useful to use thermodynamic coordinates, which like q_t (and θ for the dry system) are invariant following reversible rearrangements of fluid parcels. Typically, the choice of a coordinate carrying information about temperature is based on a moist generalization of θ. Because this generalization must specify the disposition of the state of the water mass in the reference state, two choices arise naturally: a reference state in which

$p = \pi$ and in which all the water is in the vapor state and a reference state in which $p = \pi$ and in which all the water is in the liquid state. Temperatures obtained by isentropically moving to these reference states are called the liquid water potential temperature, θ_l, and equivalent potential temperature, θ_e, respectively. By neglecting differences among the specific heats for dry air, water vapor, and liquid water, it is straightforward to show that for $q_v R_v \ll q_d R_d$

$$\theta_l \approx \theta \exp\left(\frac{-q_l L_v}{c_{p,d} T}\right) \quad \text{and} \quad \theta_e \approx \theta \exp\left(\frac{+q_v L_v}{c_{p,d} T}\right). \tag{5}$$

Although expressions more appropriate for quantitative work can be derived by not making these assumptions (e.g., Emanual 1994), the above expressions most clearly express the dominant physical processes at play and are sufficient for many purposes. From Equation 5, θ_l is readily interpreted as an evaporation temperature, which reduces to θ in the absence of condensate. In saturated conditions, the difference between θ_l and θ simply expresses the enthalpy of vaporization released through the formation of any condensation, which is responsible for constancy of θ_l. Similarly, θ_e can be interpreted as a condensation temperature. It too is invariant to changes in phase, which can be seen by noting that an increase in θ during a reversible change in phase of water is offset by a decrease in q_v (which must be equal to q_s, the saturation specific humidity) in saturated conditions. A $\{\theta_l, q_t\}$ representation of the state space provides a more nearly orthogonal basis than a $\{\theta_e, q_t\}$ representation because typically $q_l \ll q_t$. On the other hand, θ_e has the advantage of being insensitive to changes in the amount of condensate present, which motivates its use in studies of precipitating moist convection. Additionally, by replacing q_v with q_s in the definition for θ_e above, one can construct a state variable called the saturated equivalent potential temperature, $\theta_{e,s}$, whose chief virtue is that it is independent of the moisture content of the atmosphere yet is invariant following reversible displacements of saturated fluid parcels.

Compositional effects on the gas constant of the moist fluid cannot be neglected insofar as they contribute to density perturbations, where such effects are leading order. In particular, the gas constant R, which appears in the ideal gas law $p = \rho RT$ for the moist fluid, varies with the composition of the fluid according to

$$R = R_d q_d + R_v q_v = R_d(1 + q_v R_v/R_d - q_t). \tag{6}$$

Because meteorologists prefer to work with the dry air gas constant, R_d, it has become customary to define a virtual, or effective, temperature $T_v = T(1 + q_v(R_v/R_d) - q_t)$, which carries the compositional dependence of R in the moist system. Physically, T_v (or analogously $\theta_v \equiv T_v(\pi/p)^{R_d/c_{p,d}}$) is the temperature required of dry air to have the same density as moist air. Defined in this fashion, it follows that whereas for the dry system $\rho'/\rho_0 \approx -\theta'/\theta_0$, for the moist system $\rho'/\rho_0 \approx -\theta_v'/\theta_{v,0}$. However, unlike dry systems for which density perturbations can be linearly related to entropy perturbations, in the moist system, at best, one can define a piecewise linear relationship between buoyancy and state variables, depending on whether air is saturated. For instance, for a horizontally homogeneous

system whose state is described by θ_l, q_t

$$b = -g\frac{\rho'}{\rho_0} = g\begin{cases}\alpha_u(\theta_l'/\theta_0) + \beta_u q_t' & q_t < q_s \\ \alpha_s(\theta_l'/\theta_0) + \beta_s q_t' & \text{otherwise.}\end{cases} \tag{7}$$

The partial derivatives (α_u, α_s, β_u, β_s) are functions of state, which (with the help of the Clausius-Clapeyron equation) can be determined analytically. For shallow flows they are often approximated as constant, i.e., for $\theta_l = 288K$ and $q_t = 10\ \text{g kg}^{-1}$,

$$\alpha_u = 1.06, \quad \beta_u = 0.608, \quad \alpha_s = 0.49, \quad \beta_s = 3.3.$$

Compositional effects on fluid density account for the nonzero value of β_u, but the difference between the saturated and unsaturated value of the coefficients primarily encapsulate the effects of phase changes. For instance, $\alpha_s < \alpha_u$ implies that in a saturated fluid a positive perturbation in θ_l projects less strongly on to temperature (and hence density) than for an unsaturated fluid, as it is partially offset by evaporation, which cools the fluid. In contrast, because q_t perturbations induce phase changes in saturated fluids, they project strongly onto density through temperature (rather than just compositional) variations when the fluid is saturated. Although the compositional effect is usually thought to be small, over the tropical oceans it is not unusual for roughly half of the buoyancy of thermals in the unsaturated marine boundary layer to be attributable to this effect.

In general, the effect of phase changes, which is embodied in the discontinuous nature of the partial derivatives α and β (but also in other partial derivatives of the system, for instance, temperature changes along isentropes), is the origin of many fascinating aspects of moist (atmospheric) convection. Given $\{\theta_l, q_t\}$, whether a fluid parcel is saturated depends only on pressure, which (because hydrostatic pressure variations dominate) varies principally with the vertical coordinate. Thus the basic behavior of fluid parcels (as measured by their partial derivatives) depends on their position. It is almost as if the fluid is magically transformed into another form once it crosses a certain threshold. This can be thought of as a Cinderella effect, where instead of pumpkins turning into carriages and back again at a certain hour, fluid parcels change their qualitative behavior at a certain altitude. But more magical still, the witching hour (location) of each pumpkin (fluid parcel) varies with its state. In summary, moist convection can in many instances be thought of as a two-fluid problem, where one fluid (unsaturated air) can transform itself into another (saturated air) simply through a vertical displacement. This possibility greatly augments the basic anisotropy owing to gravity, which begets convection of all kinds to begin with.

A striking implication of the nonlinearity, or two-fluid behavior, embodied in Equation 7 is the concept of buoyancy reversal, wherein when dry air is mixed with saturated air of greater density it attains densities greater than those of its individual components. A common geometry for this phenomenon is illustrated in the left panel of Figure 2. Roughly speaking, buoyancy reversal occurs when there exists some mixing fraction χ such that $\rho_*(\chi) < \rho_-$, where subscript $*$ and

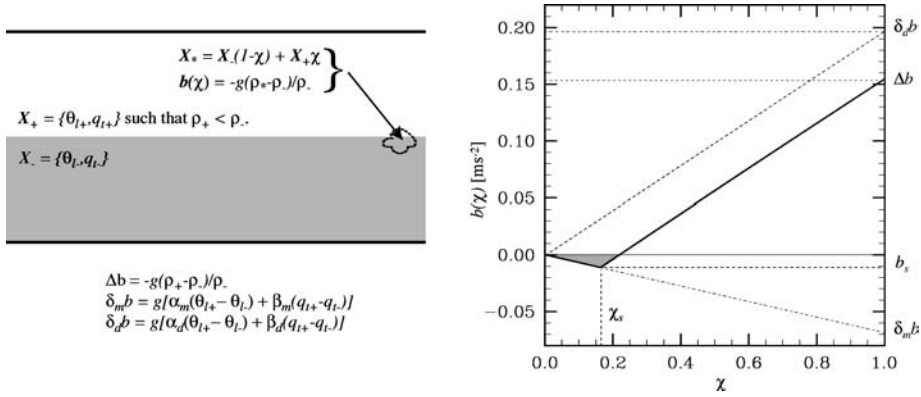

Figure 2 The right panel shows the buoyancy of a mixed parcel as a function of the mixing fraction χ at a statically stable interface between dry and saturated fluids, illustrated schematically by the left panel.

− denote the state of the mixture and the underlying air, respectively. This situation can be thought to occur when the temperature difference between the upper and lower layer is not sufficient to offset evaporative cooling, which will accompany any mixing between the two layers. At this level of approximation, this occurs whenever $\theta_{e+} < \theta_{e-}$ (+ denoting the upper, in this case dry, fluid). The inclusion of compositional effects in the equation of state results in a somewhat more stringent criterion:

$$\kappa \equiv 1 + \frac{\theta_{l+} - \theta_{l,-}}{(L/c_p)(q_{t+} - q_{t-})} = \frac{\theta_{e+} - \theta_{e,-}}{(L/c_p)(q_{t+} - q_{t-})} > \frac{c_p \theta_0}{L_v \alpha_s} \equiv \kappa_*, \qquad (8)$$

which says that whenever κ exceeds some threshold value ($\kappa_* \approx 0.2$) then some mixtures will support buoyancy reversal. How strong this effect is depends on two nondimensional numbers, κ and χ_s, the latter being the mixing fraction of the just-saturated mixture, which measures the subsaturation of the upper layer relative to the condensate available for evaporation in the lower layer. Buoyancy reversal has no counterpart in dry convection, although to the extent it is realized only under dissipative processes, it bears some similarity to double-diffusion. Situations in which buoyancy reversal is expected are commonly encountered in the atmosphere, but the role of buoyancy reversal in regulating the structure of moist convecting atmospheres remains controversial (as discussed below).

The Cinderella effect also greatly enriches conceptions of stability. With respect to infinitesimal perturbations, $\partial_z b$ still demarcates the condition of neutral stability; however, from Equation 7 it is apparent that this condition implies different relationships between $\partial_z \theta_l$ and $\partial_z q_t$ based on whether or not the fluid is saturated, which in turn depends on the amplitude of the displacement of fluid parcels. Thus the stability of the atmosphere can look different for finite amplitude, as opposed to infinitesimal, fluid displacements. Even in the isentropic limit, the stability of the fluid column has to account for the energy available to global rearrangements of fluid parcels.

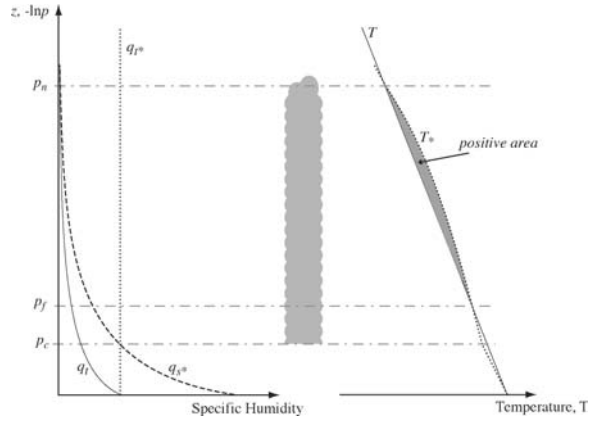

Figure 3 State diagram for an atmosphere stable to infinitesimal, but unstable to finite amplitude, displacements of near surface air.

To illustrate these types of effects, consider Figure 3. Here we describe the state of the atmosphere using the solid lines in $(q_t, -\ln p)$ space (left panel) and in $(T, -\ln p)$ space (right panel), where in the discussion that follows, z and $-\ln p$ are used interchangeably. The environmental temperature is chosen to decrease uniformly with height at the environmental lapse rate, Γ_e. The moisture field is chosen to decay exponentially such that the environment is everywhere subsaturated. In this state, the atmosphere is stable to small displacements because $\Gamma_e < \Gamma_u$, where $\Gamma_u \equiv (\partial_z T)_{\theta_l, q_t, u}$ is the temperature lapse rate for isentropic, unsaturated, vertical displacements. Because the corrections to c_p are small for an unsaturated fluid, $\Gamma_u \approx \Gamma_d \approx 10\ \mathrm{K\ km^{-1}}$.

A starting point for addressing the global stability of the atmospheric profile is the analysis of the energetics of test parcels displaced isentropically from a specified level. Such a process is labeled by subscript $*$ and illustrated by the dotted/dashed lines in the thermodynamic diagrams of Figure 3 drawn for a test parcel lifted from the surface. By definition, T_* initially decreases at the rate Γ_u with z (the height of the test parcel, whereas q_{t*} remains constant). As T_* decreases linearly with the height of the test parcel, q_{s*} decreases exponentially, rapidly attaining the value of q_{t*}. The pressure, p_c, at which they are first equal is called the lifting condensation level (or saturation pressure level), above which the test parcel becomes saturated. Further vertical displacements result in a reduced rate of temperature decline with height, according to $\Gamma_s \equiv (\partial_z T_v)_{\theta_l, q_t, s} = -g/c_*$, where

$$c_* \approx c_{p,d} \left(\frac{1 + \frac{L_v^2 q_s}{c_{p,d} R_v T^2}}{1 + \frac{L_v q_s}{R_d T}} \right)$$

is an effective heat capacity; c_* is a strong function of temperature, ranging from $2.5 c_{p,d}$ at high temperatures and asymptoting to $c_{p,d}$ as temperature decreases.

Consequently, Γ_s can be as small as 4 K km^{-1} in the lower troposphere and asymptotes to Γ_d aloft. In this example $\Gamma_u < \Gamma_e < \Gamma_s$ at the warmer temperatures of the lower troposphere, but $\Gamma_u < \Gamma_s < \Gamma_e$ aloft. Consequently, during the initial part of its saturated ascent the test parcel warms relative to the environment, whereas aloft it cools relative to the environment. Moreover, we have chosen Γ_e and q_t such that the warming above the lifting condensation level is sufficient for the parcel to become warmer than the environment (at what is called the level of free convection, p_f). As the parcel cools more rapidly with further ascent aloft, it once again attains the environmental temperature at the level of neutral buoyancy, p_n.

The distinction between the saturated and unsaturated lapse rates in the lower troposphere permits meta-stable profiles (or subcritical instabilities), as implied by Figure 3. For these situations the atmosphere is stable to infinitesimal displacements but unstable to larger displacements. This is a common situation in the atmosphere. Profiles for which $\Gamma_u < \Gamma_s < \Gamma_e$ somewhere are often called conditionally unstable, although this terminology is something of a misnomer (cf., Sherwood 2000) because even for finite displacements, whether any instability is realized depends on sufficient moisture being present for test parcels to take advantage of the favorable thermal structure of the atmosphere. For example, by sufficiently reducing the available water vapor in the profile in Figure 3, the sounding would remain conditionally unstable, but no displacement of any test parcel, finite amplitude or otherwise, would be capable of extracting energy from the mean state. Thus the convective instability is better measured in terms of the work done by a test parcel in moving from its initial position p_1 (in the above example the surface) to some final pressure level, p_2 (in the above example, p_n):

$$W(p_1, p_2) = R_d \int_{p_1}^{p_2} (T_{v*} - T_v) d \ln p. \tag{9}$$

With respect to Figure 3, $W(p_s, p_f)$ measures the negative area on the thermodynamic diagram and is called the convective inhibition (sometimes abbreviated CIN), whereas $W(p_f, p_n)$ measures the positive area (similar to what is sketched in Figure 3 but incorporating compositional, or virtual, effects as expressed by T_v) and is sometimes called the convective available potential energy, or CAPE. The presence of CIN facilitates the accumulation of CAPE, which when tapped often results in strong transient convection associated with severe weather.

Although W is frequently used as a measure of the energy available for convection, it has three major shortcomings: (*a*) it is sensitive to the starting and ending points of the test parcel; (*b*) it neglects the work demanded by continuity, i.e., the compensating motions of the environment; and (*c*) it neglects the effects of irreversible processes (ranging from precipitation to mixing) in determining T_{v*}. The first two points can be addressed by using a generalized measure of CAPE (e.g., GCAPE; Randall & Wang 1992) as follows: Let $W_{i,j}$ be a discrete version of W such that i and j index the starting and ending pressures p_i and p_j, respectively. Then $\tilde{W} = \sum_{i,j} W_{ij} P_{ij}$ defines the energy of some permutation of the system as defined

by the permutation matrix[1] P_{ij}. In an n-layer system there are $n!$ possible permutations, so if we index by k the energetic cost (reward) of the kth permutation, then generalized CAPE, or GCAPE, is simply given by $\max\{\tilde{W}_k; k = 1, \ldots, n!\} \geq 0$, where the lower bound is set by the trivial perturbation (i.e., no change). Although the generalized CAPE suffers from neither the starting point sensitivity nor the neglect of compensating motions implicit in the definition of W, it does implicitly assume (through the definition of T_{v*} in Equation 9) that rearrangements are isentropic. Both CAPE and GCAPE are limited in that they attempt to characterize with a single number the stability characteristics of the atmosphere, although the latter provides a more general framework to look at the energetics of a family of displacements (and hence things like CIN).

In constructing a language for the discussion below, I have, for the most part, focused on moist convection as an isentropic process. The buoyancy reversal argument is an argument predicated on an irreversible process; however, it is irreversible in a way that is common to most other forms of convection, namely local mixing of fluid parcels. But as illustrated below, one of the more fascinating aspects of moist convection is the varying ways in which it expresses its irreversibility. The formation of condensate not only allows for strong, local interactions with radiant energy at both terrestrial and solar wavelengths but it also leads to the formation of precipitation, which transports enthalpy across fluid trajectories. Both are long-range interactions for which there is no analog in dry convection.

3. STRATOCUMULUS CONVECTION

Stratocumulus is a low-lying, characteristically stratiform cloud type, usually exhibiting evidence of underlying cellular structure. Because moist convection is often identified with cumuliform clouds, stratocumulus is easily omitted from the canon of moist convection. This is unfortunate; not only is stratocumulus a moist convective archetype, but its driving mechanism involves precisely the type of process (radiant energy transfer) that makes moist convection so interesting. From a climatological perspective, regions where stratocumulus prevail are most evident where there exists great thermal contrast between the overlying free atmosphere and the underlying surface, for example, over the upwelling regions of the subtropical oceans, which is reflected in the right side of Figure 1, but also in the storm tracks, where in the latter they are most prevalent during periods dominated by anticyclonic circulations, and at the poles.

The tendency of stratocumulus to be most evident in subsiding maritime environments, where the thermal contrast between the surface and free atmosphere can be very pronounced, has been recognized for nearly a century. Recent studies have more systematically explored these relationships by examining the correlation

[1] A permutation matrix of an n-element set is an $n \times n$ matrix with one element of each row and one element of each column being unity and the remaining elements being zero.

between stratocumulus cloud incidence and the degree of thermal contrast between the surface and the free atmosphere, with the latter being measured by the lower tropospheric stability, defined as the difference between θ at 700 hPa and its value at the surface. Nearly two thirds of the interannual variability in the low cloud amount in the subtropical regions can be explained by variability in the lower tropospheric stability (Klein & Hartmann 1993). On shorter timescales, the variability is less, as is the fraction of the variance it can explain. Additionally, as one moves out of the heart of the stratocumulus regimes, the lower tropospheric stability becomes a less important indicator of low cloud amount, and the role of cold advection (as measured by the wind speed multiplied by the surface temperature gradient in the direction of the mean wind) becomes more important (e.g., Klein 1997). The suggestion of this analysis is that cloud amount strongly reflects the upstream conditions, indicative of memory in the system. These ideas are amplified by recent studies using satellite data (e.g., Pincus et al. 1997), which indicate that cloud amounts best correlate with conditions 24 h upstream of a given observation. In what follows, I elaborate on this statistical overview of stratocumulus and its importance by presenting an overview of important aspects of its phenomenology and the theoretical framework that has arisen to help rationalize it. A more comprehensive overview is presented by Moeng (1998).

3.1. Phenomenological Overview

Because it is relatively easy to sample experimentally, and because of its importance to the radiative balance of the planet as a whole, stratocumulus may be one of the best sampled, and best understood, if not the most recognizible, forms of moist convection. Its basic geometry is illustrated by Figure 4. Here a relatively shallow, cool, and moist thermal boundary layer is capped by a much warmer and drier subsiding atmosphere. Quantities that are invariant under displacements along isentropes (e.g., θ_l and q_t in the profiles superimposed on Figure 4) transition

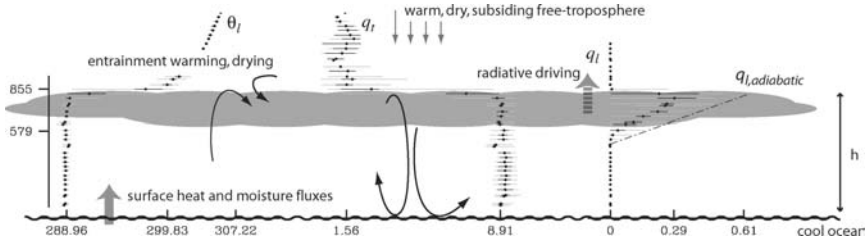

Figure 4 Cartoon of well-mixed, nonprecipitating, stratocumulus layer, overlaid with data from research flight 1 of DYCOMS-II. Plotted are the full range, middle quartile, and mean of θ_l, q_t, and q_l from all the data over the target region binned in 30-m intervals. Heights of cloud base and top are indicated, as are mixed layer values and values just above the top of the boundary layer of various thermodynamic quantities. The adiabatic liquid water content is indicated by the dash-dot line.

very sharply between their boundary layer and free tropospheric values. In the boundary layer they tend to be well mixed as a result of convective turbulence generated by infrared radiative cooling at the top of the clouds. Unlike the dry convective boundary layer, which develops from the solar heating of the land surface every day, the infrared driving of stratocumulus favors the night. This nocturnal proclivity is especially evident from five days of ship-board measurements made in regions of the south-east Pacific known to favor stratocumulus convection (Bretherton et al. 2004a).

The basic processes thought to compete in determining the thermodynamic state of stratocumulus forced in this way are also illustrated in Figure 4. Here the radiatively driven convective turbulence impinges on the cloud top interface, entraining warm and dry air from aloft. From the point of view of the mass budget, the entrainment deepening of the boundary layer works against a gently subsiding large-scale environment. The radiative cooling competes with entrainment warming and surface heat fluxes, whereas entrainment drying acts to offset the moistening effect of surface fluxes.

Because the degree to which adiabatic invariants of the flow are well mixed with height in the stratocumulus boundary layers is a foundation of many theoretical descriptions, it is important to establish the degree to which this idealization has merit. For the flight whose data is incorporated into Figure 4, this has been evaluated in several ways: by comparing the extent to which the mean cloud base, as measured by an upward-looking lidar, agrees with that predicted by the saturation pressure p_s of the state variables measured in situ below cloud base (e.g., Feingold & Morley 2003); by comparing the degree to which q_l increases with height at the rate one would expect for a layer in which q_t and θ_l are constant (illustrated by the dash-dot line in Figure 4); and by examining the extent to which rms vertical velocity maximize in the flow interior and decrease to near zero toward the boundaries (Stevens et al. 2003). By all of these measures this limit has merit.

Many studies similar to that discussed above have helped establish the canonical view of stratocumulus as a well-mixed, radiatively driven, nonprecipitating thermal boundary. Naturally, more recent work has begun to probe the limits of such idealizations, focusing in turn on when and how the well-mixed structure of the layer breaks down, how other driving forces affect the evolution of the layer, and the extent to which drizzle helps balance the water and heat budget. Despite the degree to which well mixedness serves as a useful organizing principle for understanding stratocumulus, departures from this state are not hard to find. Very early studies (e.g., Vernon 1936) documented the degree to which the diurnal variation of stratocumulus in coastal regions is accompanied by vertical stratification in state variables, with θ_l increasing and q_t decreasing with height. Aircraft measurements above the North Sea (Nicholls 1984) show that such situations are also common over the ocean and tend to be accompanied by a two-layer structure wherein a warmer, drier cloud layer is separated from a cooler, moister surface layer by a stably stratified transition layer that can be of variable depth. Such structures tend to be more evident during the day and in deeper boundary layers, and have

come to be called decoupled boundary layers. For such layers, radiative cooling from the cloud top can help maintain an elevated mixed layer that continues to dry by entrainment, but the lack of turbulent penetration to the surface cuts the cloud off from its compensating moisture supply. The development of this decoupled structure has been hypothesized to be the first step in the dissipation of the cloud layer. Its causes have been attributed to a variety of processes, including the stabilizing effect of precipitation (Paluch & Lenschow 1991, Wang 1993, Wang & Wang 1994) or solar radiation, which is preferentially absorbed in the cloud layer (Bougeault 1985, Turton & Nicholls 1987, Duynkerke 1989, Ciesielski et al. 2001).

Relatively little is known about precipitation from stratocumulus: although often idealized as nonprecipitating (e.g., Figure 4), over the years a variety of circumstantial evidence has accumulated to suggest that at times precipitation rates can be dynamically significant (e.g., Nicholls 1984, Austin et al. 1995, Bretherton et al. 1995). A surface drizzle flux of 1 mm day^{-1} will warm the boundary layer by approximately 30 W m^{-2}, which although somewhat smaller than the radiant export of energy in the nocturnal boundary layer, is commensurate with the diurnally averaged radiant export of energy. Thus it has been hypothesized that sufficient drizzle may be capable of offsetting the radiative driving of the layer, both directly and indirectly (by depleting the cloud), leading to the break up of the cloud (Paluch & Lenschow 1991). Air and ship-borne remote sensing (Comstock et al. 2004, van Zanten et al. 2005) has made possible more comprehensive surveys of precipitation in stratocumulus layers, which suggest that precipitation can be prevalent, with surface precipitation rates being most pronounced at night. Showers with rain rates of 1 cm day^{-1} are common, and precipitation rates averaged over large areas being sustained at values near 1 mm day^{-1} for many hours were observed approximately one third of the time, suggesting that drizzle may play a pivotal role in limiting stratocumulus depth. Yet more intriguing are recent observations (Stevens et al. 2005) that show that drizzle seems to be connected to the emergence of pockets and perhaps even broader regions of open cellular convection embedded in otherwise more overcast cloud regions—a striking example of which is shown in Figure 5.

One of the more vexing problems pertaining to stratocumulus convection is how and why the stratiform cloud layer breaks up into more broken or scattered convection, as is characterized by the downstream transition in low-level cloudiness in Figure 1. One idea is that as the stratocumulus layer advects over warmer water, the thermal contrast across the boundary layer is reduced, whereas the moisture contrast is enhanced, leading to an increased potential for buoyancy reversal (e.g., as measured by κ in Equation 8). In the buoyancy reversal regime, mixing with the free troposphere is argued to induce further mixing, promoting the destruction of the cloud. This idea, first stated in the 1960s (Kraus 1963, Lilly 1968) is best known as the cloud top entrainment instability (CTEI) hypothesis, a term that was coined after it was refined to account for compositional effects on buoyancy (Deardorff 1980, Randall 1980). Early tests showed that regions of stratiform

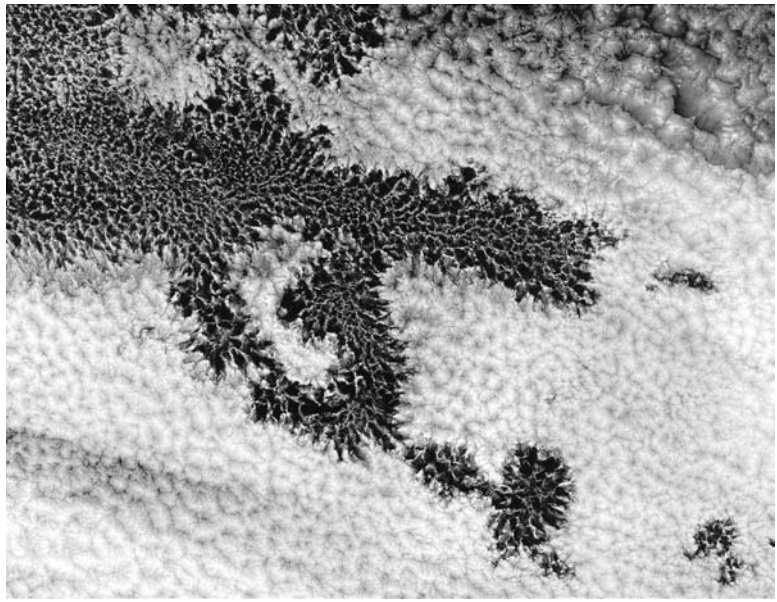

Figure 5 Example of a region of open cellular convection (*dark cell interiors, with bright cell walls*) embedded in a broader region of closed cellular convection (*bright cells with darkened cell walls*). Open cellular regions have scales ranging from 5–50 km and have been hypothesized to be envelopes where drizzle is more prevalent.

clouds were prevalent in conditions where the CTEI hypothesis would predict their demise (Kuo & Schubert 1988, Albrecht 1991), leading to refined arguments and more stringent criteria for cloud dissolution (MacVean & Mason 1990, Siems & Bretherton 1992, Duynkerke 1993). Although none of these measures has proven to provide a compelling ordering of the data, the more stringent criteria tend to perform better. More recent observational data (De Roode & Duynkerke 1997) and simulations (Lewellen & Lewellen 1998, Moeng 2000) lead to renewed interest in the original CTEI formulation, but analysis of yet more recent measurements for which $\kappa > \kappa_*$ is accompanied by a thickening of the cloud seems to indicate that at the very least CTEI is not a sufficient condition for cloud desiccation (Stevens et al. 2003).

In the past decade, theoretical work (Krueger et al. 1995, Bretherton & Wyant 1997, Stevens 2000, Lewellen & Lewellen 2002) has turned away from CTEI and begun to focus on a broader account of the energetics, hypothesizing instead that as nonradiative forcings begin to dominate the energetics of the stratocumulus-topped boundary layer the cloud can begin to entrain sufficiently large amounts of air to negate the radiative cooling, thereby requiring work to mix the entrained air below the cloud base. The concept of the cloud layer needing to do work on the subcloud layer to maintain a well-mixed layer (elegantly illustrated by

Schubert et al. 1979) arises from the two-fluid nature of moist convection embodied in Equation 7. In such a situation, the circulation should transition from an overcast stratocumulus-like circulation to a more cumulus-like circulation wherein the downward mass flux is predominately unsaturated. Consistent with the observations, a variety of factors can influence this change, ranging from the state of the cloud top interface, to precipitation, solar radiation, enhanced cloud base warming by longwave radiative fluxes, and enhanced sensible and latent heat fluxes, some of which (surface latent heat fluxes and cloud base radiative warming) are particularly prevalent for deeper boundary layers.

3.2. Theoretical Perspectives

The theoretical foundation of our understanding of stratocumulus is Lilly's (1968) mixed-layer theory. By integrating over the boundary layer (e.g., from $z = 0$ to h in Figure 4), and by assuming a well-mixed vertical structure, it is possible to describe the evolution in terms of a system of three ordinary differential equations:

$$\frac{D}{Dt}h = W + E \tag{10}$$

$$\frac{D}{Dt}\hat{\theta}_l = -\Delta F + V(\theta_{l,0} - \hat{\theta}_l) + E(\theta_{l,+} - \hat{\theta}_l) \tag{11}$$

$$\frac{D}{Dt}\hat{q}_t = -\Delta R + V(q_{t,0} - \hat{q}_t) + E(q_{t,+} - \hat{q}_t), \tag{12}$$

where hats denote the vertical average of variables (i.e., $\hat{\theta}_l = 288.96$ K and $\hat{q}_t = 8.91$ in Figure 4), and subscripts 0 and 1 denote values of state variables at the surface and just above the boundary layer, respectively. The substantial derivatives D/Dt denote a change following the mean horizontal flow, whereas ΔF and ΔR are sources of θ_l and q_t, respectively; W is the large-scale vertical motion field; V is a surface exchange velocity used to parameterize the surface fluxes; and similarly E parameterizes the entrainment fluxes. With V determined by a surface-exchange law, all that remains to close the theory is to determine E. Just how to do this has been, and remains, a topic of great interest.

A starting point for evaluating E is the energetics of stratocumulus-topped boundary layers. Such an approach takes advantage of a feature of the mixed-layer theory in that the assumption on the vertical structure allows one to consistently couple the energetics of the flow (as measured by the buoyancy flux, $\mathcal{B} \equiv \overline{w'b'}$) to the evolution of the mean state. This becomes evident by noting that the necessary condition for a mixed layer to remain well mixed is for the sum of the diabatic and turbulent fluxes of a state variable to be linear. That is, for a horizontally homogeneous flow,

$$\partial_t \overline{\theta}_l = \partial_z \left(\overline{w'\theta'_l} + F \right); \tag{13}$$

then for $\partial_t \partial_z \theta_l$ to vanish, $(\overline{w'\theta'_l} + F)$ must be a linear function of z. Such a situation

is referred to as a quasi-steady state. Given a knowledge of the diabatic forcings F and turbulent fluxes at the flow boundaries (which are given if E and V are known), quasi-stationarity determines the structure of $\overline{w'\theta_l'}$ in the flow interior. Because similar relations constrain $\overline{w'q_t'}$, the resultant profiles of the turbulent fluxes of q_t and θ_l can be used to determine $\mathcal{B}$, given Equation 7.

A variety of approaches have been used to determine E as a function of $\mathcal{B}$. Most initial work made closure assumptions for E in analogy to the dry convective boundary layer, for instance, by choosing E such that $\mathcal{B}_{\min}/\mathcal{B}_{\max}$ is some fixed ratio, or so that the integral of $\mathcal{B}$ over its negative area is some fixed fraction of its integral over its positive area (Schubert 1976, Kraus & Schaller 1978). Inspired in part by large-eddy simulation, it has gradually come to be realized that constraints on the net buoyancy flux poorly bound the energetics of the flow, and that a more useful approach is to fix E by requiring that ratio of $\mathcal{B}$ to its value for a hypothetical, nonentraining flow be fixed (Manins & Turner 1978, Stage & Businger 1981, Lewellen & Lewellen 1998, Lock 1998, van Zanten et al. 1999). Exactly how best to count the energetics is complicated by uncertainty about how to best account for diabatic fluxes that occur in the entrainment zone (e.g., Moeng et al. 1999, Moeng & Stevens 1999), as well as how to relate fluxes of conserved variables to $\mathcal{B}$ at partially saturated interfaces such as cloud top (Lilly 2002, Randall & Schubert 2004). Many recent closure hypotheses for E have been calibrated using large-eddy simulation, but the ability of this approach remains controversial, in part because entrainment rates from LES can vary substantially from model to model and as a function of the representation of the cloud top interface (Stevens 2002, Stevens et al. 2003). Despite significant uncertainty, a variety of recent work (ranging from observations of pronounced drizzle to direct measurements of entrainment) seems consistent with the idea that entrainment in stratocumulus-topped mixed layers is less efficient than predicted by many of the early closures.

Notwithstanding some vexing problems and ready complications, idealized stratocumulus flows are arguably the form of moist convection most analogous to common forms of dry convection. For instance, the simplest stratocumulus flow could consist of a saturated fluid bounded above and below and driven by fixed-buoyancy fluxes. Such a problem is isomorphic to the Rayleigh-Bénard problem for dry convection. Beginning with this problem, gradual steps toward more realistic stratocumulus layers could be made by studying the dynamics of partially saturated layers, in which case the nondimensional cloud base height and the relative driving of q_t and θ_l fluxes to the flow enter as two nondimensional numbers. In the limit of the saturated fluid consisting of infinitely small and numerous drops, one could pose the problem in a way that is tractable for direct numerical simulation. By prescribing the boundary forcings, this approach avoids dealing with the critical issue of entrainment; nonetheless, it can provide interesting and important insight into the dynamics of stratocumulus layers. Despite its simplicity and relevance, very little research of this kind has taken place. It would seem to be a natural entry point for those from the broader fluids community who are looking to bring their expertise and creativity to meteorological flows.

4. SHALLOW CUMULUS CONVECTION

Shallow cumulus convection is ubiquitous. It spans large expanses of the world's oceans, and it is common over land during the day in periods when fair weather prevails. From a popular perspective, it is the archetypical form of moist atmospheric convection, although as compared to other forms of convection, it is relatively infrequently studied. Its diminutive size (and hence radiative impact) and tendency not to be associated with precipitation renders it less studied than either stratocumulus or deep precipitating convection. In Figure 1, it is represented by the middle portion of the circulation as isolated cumulus drafts confined to the lower troposphere. In this context, it is often referred to as trade-wind cumulus convection and is seen as a structural component of the thermal boundary layer in the trades. If the various modes of convection were drafted in proportion to their frequency of occurrence, the shallow regime would occupy most of the figure.

The motivation for studying shallow convection stems from an early recognition of its role in maintaining the structure of the lower troposphere in the trades and hence the intensity of large-scale circulations in the tropics (Riehl et al. 1951). The trade-wind structure is most significantly marked by the presence of a "trade-wind inversion," which is a zone of increasing temperatures usually found somewhere between 1 and 2 km above the surface. Although it tends to be weaker and more variable than its counterpart capping stratocumulus, the trade-wind inversion also caps cloud development (albeit less decisively), thereby marking a transition between warm and dry free-tropospheric air and the cooler, moister turbulent boundary layer. It is ubiquitous in the trades (von Ficker 1936, Neiburger et al. 1961); similar features are sometimes evident between periods of precipitating convection in the deep tropics (Nicholls & LeMone 1980, Johnson & Lin 1997). Studies have long argued that the maintenance of this inversion structure is accomplished through the action of shallow cumulus, which moisten and cool the subsiding free atmosphere (e.g., Nitta & Esbensen 1974), thereby accumulating the large amounts of latent heat in the lower troposphere necessary to feed regions of deep precipitating convection and drive associated large-scale circulations (e.g., Riehl et al. 1951, Tiedtke et al. 1988). The following sections briefly discuss the phenomenology and theory of shallow cumulus convection in the trades, with an eye toward recent developments. Excellent, and more comprehensive, reviews on this topic are given by Betts (1997) and Siebesma (1998).

4.1. Phenomenological Overview

The mean structure of the atmosphere in regions where shallow convection prevails is illustrated by the schematic in Figure 6. Many elements of the mean structure were described on the basis of aircraft observations quite early, most notably in a remarkable body of work by Malkus (1954, 1956, 1958). The mean structure in the cartoon is derived from large-eddy simulation, but it well illustrates many generic features of the trade-wind boundary layer: (*a*) A well-mixed subcloud

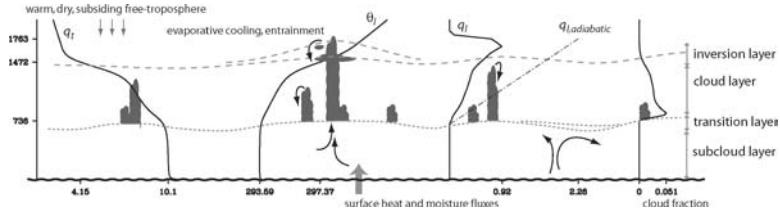

Figure 6 Cartoon of trade-wind boundary layer from large-eddy simulation. Heights of cloud base, level of maximum θ_l gradient (inversion height), and maximum cloud penetration depth are indicated, as are subcloud layer and inversion-level values of thermodynamic quantities. Cloud water contents are averaged over cloudy points only, with adiabatic liquid water contents indicated by the dash-dot line. The far right panel shows cloud fraction, which maximizes near cloud base at just over 5%.

layer extending to cloud base; (*b*) a transition layer of 100–300 m in depth, which is best defined in terms of the changing moisture field, but also evident as a layer of weak stability and maximum wind speeds; (*c*) a conditionally unstable cloud layer spanned by cumuliform clouds whose area coverage is typically less than 10%; and (*d*) an inversion layer of several hundred meters in extent that caps the clouds and separates the thermal/moisture boundary layer from the overlying free atmosphere. This structure is also illustrated from the 915-Mhz reflectivity signal from an upward-pointing radar in Figure 7. The tendency for clouds to be confined to a relatively shallow layer (less than 2 km) and their short lifetime is thought to inhibit the formation of precipitation, and for the most part shallow cumulus convection has come to be synonymous with nonprecipitating cumulus convection (Betts 1973). Unlike other forms of moist convection for which important aspects of

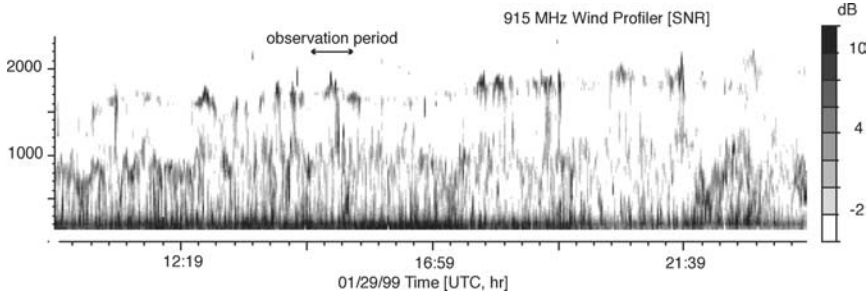

Figure 7 Signal-to-noise ratio from a 915-Mhz wind profiler. At this wavelength, Bragg scattering from humidity gradients dominate the signal, thus illustrating the turbulent structure of the trade-wind boundary layer by highlighting regions of vigorous mixing associated with subcloud thermals and cloud boundaries. Both the trade-inversion and transition layer are evident at this frequency. (Adapted from Kollias et al. 2001.)

their description requires energy to be transported across flow streamlines, either by falling hydrometeors or by photons, in its ideal form, shallow cumulus convection acts irreversibly only through local mixing with its environment; in this sense, it is similar to dry convection. It differs from both dry convection and stratocumulus convection primarily in its inherent asymmetry of up- and downward motions. Upward currents are more likely to be saturated and extract energy from the flow, downward currents tend to be unsaturated and must do work on the flow—this "up-moist, down-dry" asymmetry in the mean, cloud-scale, motion field has long been thought to be why cumulus clouds tend to have small area fractions (Bjerknes 1938).

Over the ocean the depth of the subcloud layer is relatively constant; cloud base is usually found between 600–800 m above sea level (Betts & Albrecht 1987). Its turbulent structure is remarkably similar to that found in the dry CBL: The flux of buoyancy normalized by its surface value ($\mathcal{B}_0$ decreases from unity at the surface to a value near $-1/5$ at the top of the subcloud layer; and fluctuations of the vertical velocity tend to be well scaled by a convective velocity scale $w_* = [\mathcal{B}_0 h]^{1/3}$ (Deerdorff 1970). Such relationships are evident both in observations and simulations (Nicholls & LeMone 1980, Stevens et al. 2001, Siebesma et al. 2003). There are, however, indications that momentum and moisture fluxes are enhanced under patches or lines of active convection, and of cloud "roots" extending 100 m or more into the top of the subcloud layer (LeMone & Pennell 1976, Nicholls & LeMone 1980, Ötles & Young 1996). Such features are indicative of underlying support for developing cumulus elements and are evident in cross-sections of the turbulent circulation derived from LES, but their implication for modeling and theoretical work remains unclear. As for the patterns of organization of the cloud field, although the role of mean wind in developing boundary layer rolls and cloud streets has been the focus of many studies, relatively little attention has been devoted to the mechanisms for clustering on scales of 50 km or so (Malkus 1958, LeMone & Pennell 1976). Although usually idealized as nonprecipitating, there is ample evidence of precipitation from shallow convection (Short & Nakamura 2000), raising the question as to whether this often-neglected process might play a critical role in the organization and other elements of shallow cumulus convection (see also Jensen et al. 2000).

The role of the transition layer in regulating trade-wind convection remains controversial. Typically, it varies from 100–300 m in depth and is most evident by a decrease in q_v by more than 1 g/kg, and to a lesser extent a slightly enhanced lapse rate of θ. In a recent study of soundings from the Eastern tropical Pacific, transition layers were evident roughly 45% of the time (Yin & Albrecht 2000). Spatial variations on the cloud-separation scale (order kms) tend to wash out its structure in the mean profiles in Figure 6. A more marked structure would be evident in individual vertical profiles from the large-eddy simulation. Its ubiquity has led to speculation about its dynamic role (e.g., Yin & Albrecht 2000, Stevens et al. 2001). However, the incorporation of such a layer into theories of trade-wind cumulus has been spotty, indicative of the lack of consensus in this respect.

Past studies of nonprecipitating cumulus convection tend to focus predominantly on the structure of clouds (as test parcels or families of test parcels), and to a lesser extent on the structure of the cloud layer. This distinction is somewhat analogous to the differences between CAPE and GCAPE, where the latter views clouds as just one part of a global rearrangement of the fluid. An excellent, and still current, review of the structure of individual clouds is given by Blyth (1993). Some consensus characteristics of clouds summarized at that time include (*a*) well-defined clouds boundaries; (*b*) the tendency for updrafts to be concentrated within the cloudy envelope and downdrafts to predominate around the edges of the cloud, especially near the cloud top; (*c*) similar cloud and environmental lapse rates; and (*d*) heterogeneous cloud properties indicative of active mixing between the clouds and their environment. To this could be added the tendency for turbulence to be concentrated in the clouds and their near fields. Blyth's review primarily summarized information gleaned from decades of in situ cloud measurements. In the decade since, our understanding has advanced most rapidly as a result of improved remote sensing capabilities and large-eddy simulation. Figure 8 from Kollias et al. (2001) shows the tendency for updrafts to penetrate into the stably stratified air capping the cloud layer, with maximum vertical velocities greater than 5 m s^{-1} and downdrafts of nearly -3 m s^{-1} crowning the cloud top. Regions of active mixing, in this case measured by the spreading of the Doppler spectrum, tend to locate near cloud edges.

Another view of the structure of the cloud layer is provided by the distribution of state variables $\{\theta_l, q_t\}$ at a fixed pressure level within the cloud layer, as shown in Figure 9 (Neggers et al. 2002). For this pressure level, the temperature at which $q_t = q_s$ is represented by the dash-dot line, and the line of neutral buoyancy whose slope changes in the saturated versus unsaturated region of state space (cf., Equation 7) is indicated by the dashed line. This division separates the plane

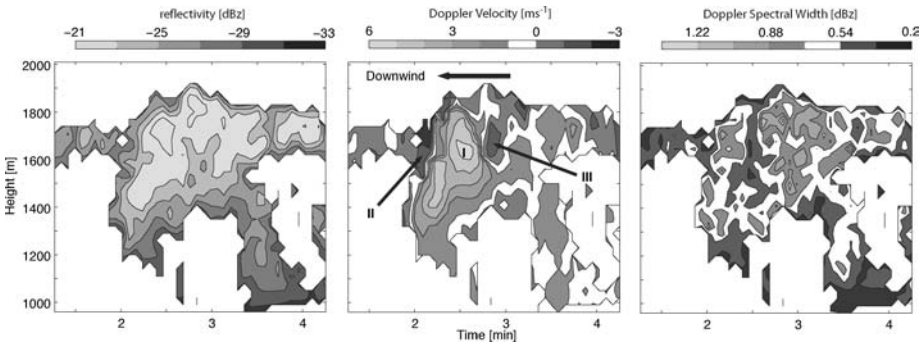

Figure 8 Radar reflectivities (*left*), Doppler velocities (*center*), and Doppler spectral width (*right*) for a cumulus cloud sampled during the observational period marked in Figure 7. Updrafts and downdrafts are marked on the central panel. Notice the rather broad spectral widths in the updraft core in the rightmost panel. (Adapted from Kollias et al. 2001.)

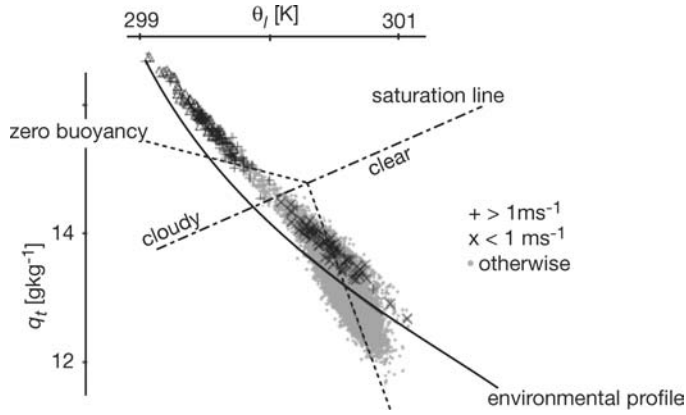

Figure 9 Distribution of state variables on a $q_t - \theta_l$ diagram for a fixed level within the cloud layer as derived from LES and first published by Neggers et al. (2002). The environmental profile shows the change in the mean state with height; the mean value at the given height is indicated by the intersection of the environmental and zero-buoyancy line. Points above or to the right of the zero-buoyancy line are positively buoyant, points below or to the left are negatively buoyant. The kink at the intersection with the saturation line reflects the change in buoyancy for the saturated versus the unsaturated fluid. Note that strong updrafts are rare, cloudy, and buoyant.

into four quadrants: positively buoyant saturated air on the upper right, positively buoyant unsaturated air on the lower right, negatively buoyant saturated air on the upper left, and negatively buoyant unsaturated air on the lower left. The symbols also separate the air into strong updrafts, strong downdrafts, and environmental air. The tendency of updrafts to be relatively rare, saturated, and positively buoyant, whereas downdrafts are subsaturated and negatively buoyant, is clearly evident (although the symbols separating up- and downdrafts are difficult to make out). The strong drafts almost appear to be drawn from a distinct population relative to the more Gaussian spread of the background flow, which we take as being further indicative of the two-fluid nature of the problem, as per Section 2.2. The degree to which updrafts are moister and cooler (in the sense of θ_l) than the environment also emphasizes their role in the transport of heat and moisture through the layer. This latter property helps motivate the atomistic view of clouds emphasized by the mass flux methodology discussed below.

The necessity of considering the cloud field as an ensemble of drafts is emphasized in Figure 6. Here, increased gradients of q_l within the inversion layer and the very small values of cloud fraction at this height are indicative of the role of relatively rare and strong plumes in penetrating into the stably stratified environment. The decreasing cloud coverage with height suggests that most clouds penetrate through the depth of the cloud layer for a relatively short period of their lifetime, if ever. Attempts to quantify this distribution find that the probability, p, of finding

a cloud of scale ℓ (associated with the square root of cloud area projected to a horizontal plane) is a power law of the form $p(\ell) = a\ell^b$, with $-2 < b < -5/3$ up until a scale break at some size ℓ_c. Clouds with size $\ell > \ell_c$ are relatively rare (Plank 1969, Benner & Curry 1998, Neggers et al. 2003). This scaling implies order ℓ_c clouds dominate the area coverage, and although not obvious (but related to the tendency of larger clouds to have more vigorous mean updrafts), these clouds are even more dominant from the point of view of energetics. Thus the scale break is a controlling parameter of the cloud size distribution. What determines this has been a matter of speculation, but the depth of the cloud and subcloud layer are obvious candidates (Neggers et al. 2003). Simulations have also argued for a scaling of cloud perimeter area versus volume, implying a fractal dimension of 7/3 for cloud surface area, consistent with observational analyses of area, perimeter length, and scalings from observations (Siebesma & Jonker 2000), all of which point to the cloud field being rich in scales, an idea in accord with even the most casual observation of the untrained eye.

4.2. Theoretical Perspectives

Theoretical work has tended to focus on models of the cloud elements as a function of the mean state. Given a mean field ϕ (usually taken to be either θ_l or q_t), its evolution owing to moist convection can be written as

$$\partial_t \phi|_{\text{clouds}} = -\partial_z F^\phi, \tag{14}$$

where F^ϕ is a turbulent flux largely identified with the clouds. From this point of view, the job of a cloud model is to specify the flux. Much recent work has adopted the "mass flux" perspective (Asai & Kasahara 1967),

$$F^\phi = \frac{M}{\rho}(\phi^c - \phi), \tag{15}$$

where M is the mass flux carried by the clouds, ρ is the density, and $\phi^c - \phi$ measures the difference between cloud-averaged values of ϕ (denoted by superscript c) and their environmental values (see Tiedtke 1989, Siebesma 1998 for an application of these ideas to nonprecipitating shallow convection). In the sense of Figure 9, this is as if the flux is entirely carried by a single plume whose properties are identical to those obtained by conditioning the average over just cloudy, or perhaps buoyant and cloudy, parcels. On the basis of such an averaging procedure, one can derive equations for M and ϕ^c:

$$\partial_z M = (\epsilon - \delta)M \tag{16}$$

$$\partial_z \phi^c = -\epsilon(\phi^c - \phi). \tag{17}$$

Here two inverse-length scales, ϵ and δ, determine the change of M with height. Physically, they are interpreted as the rate at which the cloud ensemble is diluted through the incorporation of environmental air (cf., Equation 17) and diminished

through the detrainment of cloud mass. Although Equations 16–17 make ready reference to physical processes, such as entrainment and detrainment, the specification of ϵ and δ is equivalent to specifying the nondimensional profile of M and ϕ^c (Bellon & Stevens 2005).

Closure of the above system requires a specification of $\{\epsilon, \delta\}$, boundary conditions that determine M and ϕ^c at cloud base, and some means for determining the support of F^ϕ, i.e., the depth of the cloud layer. The model (Equations 16 and 17) differs from a similarity plume through the inclusion of δ, which arises when one associates M with an ensemble of drafts. (For single-plume models, detrainment also occurs, but by definition only catastrophically at cloud top.) Recently, however, the similarity plume approach has been reemphasized but for a distribution of plumes, each of which satisfies Equation 17, chosen to span the distribution of cloudy elements (Neggers et al. 2002, Cheinet 2004). In such an approach, the number of cloudy plumes and their respective updraft velocities, typically modeled using a simplified momentum equation (e.g., Simpson & Wiggert 1969, Siebesma et al. 2003), implicitly determines the vertical profile of M. The bulk and multiparcel approaches share a common need to model ϵ. Similar to the entrainment problem for stratocumulus, this is a central and long-standing problem in the modeling of cumulus clouds, for which many ideas (Raymond & Blyth 1986, Siebesma & Cuijpers 1995, Siebesma 1998, Cheinet 2004) have been proposed. Although there is an emerging consensus that cumulus drafts entrain more rapidly than similarity arguments would seem to indicate (largely based on an analysis of large-eddy simulation, e.g., Siebesma & Cuijpers 1995), little consensus has developed around any specific approach. Simulations have also been used to evaluate closure assumptions for M and ϕ^c at the cloud base. Typically, ϕ^c is associated with the statistics of the subcloud layer, whereas if the atmosphere is determined to be convecting, M is determined in a variety of ways, most typically through a constraint on the subcloud layer (Albrecht et al. 1979, Tiedtke 1989, Grant 2001). Here, however, there does appear to be an emerging consensus that the cloud base value of M scales with w_*, as initially argued by Nicholls & LeMone (1980).

With most research focusing on a description of the cloud layer, relatively little work has addressed the broader question of how clouds help maintain the observed boundary layer structure. Numerical experiments (McCaa & Bretherton 2004) suggest that cumulus-induced deepening of the layer is crucial in mediating the observed transition between regions of more stratiform clouds and the more broken trades. However, most models of cumulus convection neglect any explicit consideration of the interaction of the cumulus layer with the overlying free atmosphere, although this (in the end) will determine the statistics of the cloud layer. Betts & Ridgway (1989) proposed a simple steady-state theory of the trade-wind boundary layer that only incorporates the cumulus dynamics in so far as they determine the mean structure of the cloud layer; energetically, such a model is constrained by the heat balance of the subcloud layer. A two-layer model developed by Albrecht et al. (1979) attempts to more formally incorporate cloud processes into

its dynamics; however, in addition to being sensitive to parameters whose values are difficult to constrain (Bretherton 1993), it was recently pointed out that this framework rests on assumptions about the cloud layer structure that are inconsistent with the assumed model of mixing (Bellon & Stevens 2005). These frameworks are also difficult to close because for partially saturated layers, relationships similar to Equation 7 depend on the full joint pdf of thermodynamic state variables (Bechtold & Siebesma 1998). Although some recent work has attempted to unify the representation of cloud and subcloud processes (Lappen & Randall 2001, Golaz et al. 2002a,b, Cheinet 2003, 2004), these models require a vertically resolved representation of the trade-wind layer. Overall, efforts to understand trade-wind cumulus convection remain hampered by the lack of a compelling representation of the bulk structure of the trade-wind layer that is capable of consistently incorporating more sophisticated statements of cloud processes, for instance, as represented by the models discussed above.

Another approach to studying trade-wind clouds has been to study their similarity structure, which is analogous with the study of dry convective boundary layers (Grant & Brown 1999, Brown & Grant 2000). The evolution of shallow cumulus as air advects downstream over warmer water in the trades has much in common with the growth of the dry convective boundary layer. Recently, Stevens (2004) proposed a framework for studying trade-wind cumuli wherein the cloud layer grows into a layer with a fixed lapse rate of θ_v in the free troposphere, an exponentially decaying initial moisture profile, and a sea-surface temperature that is continually adjusted to maintain a constant surface buoyancy flux. Even with a paucity of additional parameters (the moisture scale height, decay scale, and initial value) this problem is difficult to constrain by similarity approaches. From the point of view of large-eddy simulation, one finds that initially the boundary layer depth increases with time, t, following the square-root law $h \sim t^{1/2}$, as would be expected from similarity arguments for the analogous problem in dry convection. But with the onset of moist convection we find that $h \sim t$. Because the flux of condensed water into the inversion layer can be expected to depend linearly on cloud depth, such a model is consistent with the longstanding view of trade-cumulus maintaining the depth of the trade-inversion by evaporating cloud water into it. Results from this analysis also show that the proportionality scaling between cloud base mass flux and w_* proposed by Nicholls & LeMone (1980) well represents the variability in the data.

5. DEEP PRECIPITATING CUMULUS CONVECTION

Among students of convection, atmospheric moist convection is often identified with deep precipitating cumulus convection (cumulonimbus), as sketched over the warm water segment of Figure 1. Because deep cumulus convection is so strongly associated with precipitation, the statistics of the latter often serve as a surrogate for the former. From this perspective, we have learned that deep precipitating

cumulus convection is a relatively rare phenomena. Early work hypothesized that roughly 2000 hot towers (i.e., nondilute cumulonimbus clouds stretching to the tropopause) whose areal coverage is less than 0.5% are all that are necessary on a daily basis to satisfy the energy balance of the equatorial trough (low-pressure) zone. Satellite studies suggest that actual precipitation zones tend to be more extensive but still highly textured in space and time. Statistically, they correlate well with oceanic regions where sea-surface temperatures are warmer than 27°C–28°C, surface winds are convergent, and a bulk measure of the atmospheric relative humidity is high (Bretherton et al. 2004b). Budget studies show that the diabatic processes associated with cloud processes in these regions tends to warm and dry the troposphere, with most of the drying being concentrated below the freezing level (roughly 5 km) and most of the warming being evident at higher levels (Yanai et al. 1973). These patterns of heating and moistening are consistent with two dominant modes of convection, one shallow and nonprecipitating, another deep and precipitating. Because the impact of such diabatic processes feeds back strongly on adiabatic circulations (Reed & Recker 1971, Emanuel et al. 1994), it is more difficult to separate deep moist convection from its environment, as is commonly done for nonprecipitating convection. Such difficulties are reinforced by noting that although deep convection tends to locate in flows whose adiabatic component is upwelling, these same budget studies suggest that the net mass flux in ascending branches of large-scale circulations is less than the upward mass fluxes within the cumulus clouds themselves. Given that the area-fraction of deep convection is relatively small, this explains why most of the air in the ascent regions of the tropics is actually descending.

This early view of tropical convection, and hence precipitation systems, emphasized what can be thought of as a precipitating version of Figure 6, wherein the trade-inversion is displaced to the tropopause and isolated cumulonimbi span the depth of the troposphere (12–18 km), producing copious amounts of surface precipitation and perhaps a cirroform cloud shield (Riehl et al. 1951). Despite the grip this view maintains on the community's collective imagination, on the basis of early radar and satellite measurements, airborne photogrammetric studies, and in situ measurements, it has long been apparent that much of the deep convection over oceanic regions is intricately structured with dynamically coherent lines or clusters on scales ranging from hundreds to thousands of kilometers (Zipser 1969, Nakazawa 1988; see also the review by Zipser 2003b). Moreover, many of these early studies showed that a significant fraction (if not most) of the precipitation associated with such organized systems had a more stratiform radar signature (Houze 1997), suggesting that naive associations between tropical preciptiation and deep convection are flawed, and that an understanding of precipitating deep convection must address the interplay between its more convective and stratiform components.

More recent and systematic studies suggest that convective cells and the more stratiform regions of precipitation, which often accompany organized clusters of such cells, are each responsible for commensurate amounts of tropical precipitation, roughly 40% each, with the remainder associated with "shallow" systems.

The two classes of precipitating convection have distinct spatial statistics: Convective regions tend to be more frequent, cover less area, and precipitate much more vigorously (by a factor of four or greater) than their stratiform counterparts, all of which is consistent with such regions having a greater convective intensity (Schumacher & Houze 2003, Nesbitt et al. 2000). Stratiform regions tend to have a more pronounced diurnal cycle (over the ocean), with area-fractions and mean sizes increasing at night (Nesbitt & Zipser 2003), consistent with them being more influenced by radiative processes (cf., Section 3). Although larger-scale organization appears to be endemic to moist atmospheric convection, it is perhaps the most difficult to ignore for the case of deep convection, even more so for maritime deep convection where even the prevalence of tropospheric-spanning hot towers has recently come into question (Zipser 2003a). This is not to say that deep cumulonimbus clouds do not exist, rather that their idealization as undilute towers that penetrate an otherwise blue sky to vigorously transport boundary layer air directly to the tropopause has proven too simplistic. For this reason, and because the deep (albeit dilute) convective cells that do exist are essential to the development of regions of stratiform precipitation, below I review our current understanding of deep, maritime convective cells as seen from the perspective of recent observational and modeling studies. Further background is provided in the texts by Cotton & Anthes (1989), Houze (1993), and Emanuel (1994). For the case of convective systems with meso- (or larger) scale organization, refer the reader to reviews by Redelsperger (1997) and Houze (2004).

5.1. Phenomenological Overview

To the extent that deep moist convective cells resemble extended versions of their counterparts in the trades, many of the concepts from the previous section are relevant to deep convection as well. For instance, recent work has begun to focus on the interactions of deep convection with the upper troposphere and lower stratosphere leading to the development of a tropical tropopause layer (indicated roughly by the dashed lines above the regions of deep convection in Figure 1), which in some sense is thought to be analogous to the entrainment/inversion layer capping trade-wind clouds (Sherwood & Dessler 2001). Although many analogies exist, the depth of the convecting layer introduces new phenomena, including precipitation, which transports enthalpy across fluid stream lines; ice-microphysics, whose nonequilibrium behavior influences precipitation formation and interacts strongly with radiant streams of energy; and more disparate timescales for moisture and temperature profiles to adjust to the convection.

Like the shallow convecting layers, layers of deep convective clouds exhibit a spectrum of cloud types. Aircraft and radar studies based on data collected during the Atlantic Tropical Experiment of the Global Atmospheric Research Program (GATE) suggest that the spectrum of clouds is lognormally distributed, whether they are measured in terms of radar reflectivities, updraft area, intensity, or mass flux (e.g., López 1977, LeMone & Zipser 1980). Notwithstanding the evidence for

a broad spectrum of cloud types, much theoretical work is based on a categorization of discrete modes. As a result of the early budget studies, the emphasis has been on two modes: deep and shallow convection, although recent work has sought to emphasize the importance of a midlevel congestus mode thought to account for roughly 20% of the observed precipitation (Johnson et al. 1999, Tung et al. 1999), a point of view rationalized by the presence of three distinguished layers in the troposphere: the trade-wind inversion, a freezing-level stable layer, and the tropopause.

There is also evidence that the structure of maritime cumulus convection changes as the depth of the convecting layer becomes deeper. In particular, maximum updraft velocities stop increasing as the clouds extend above 3 km and the ratio of observed liquid water to adiabatic liquid water becomes more approximately constant. During GATE, maximum updraft velocities tend to be less than 5 m s^{-1} and hardly ever exceed 10 m s^{-1} (LeMone & Zipser 1980). On average, the mean diameter of convective elements (roughly 1 km) does not appear to vary greatly with height, and like trade cumulus, they tend to cover less than 5% of the available areas. Likewise, θ_v perturbations tend to be approximately 0.5 K, irrespective of height, indicative of active mixing (Zipser & LeMone 1980). As is the case for shallow convecting layers, downdrafts in deep convecting layers tend to be weaker and shallower than the updrafts (cf., Figure 8). However, the evaporation of precipitation drives downdrafts in the intercloud environment, which are an important component to the balance of heat, moisture, and mass within the convecting layer (Johnson 1976). Moreover, because shafts of precipitation falling through the updraft can make the cloud collapse, the trajectory of the precipitation and the tilt of the cloud have a strong influence on the convective lifecycle. Because both are determined in part by the profile of the environmental wind, the development of precipitation provides additional pathways for the mean wind to organize convection, this being a particularly rich and active area of research that has little in common with studies of the organization of dry or nonprecipitating convection through the interplay between buoyancy and wind shear. These effects of precipitation, and the radiative effects of ice-processes, further complicate attempts to measure the stability of the atmosphere based on the displacements of test parcels (e.g., Section 2.2).

One question, which although relevant to shallow, becomes more pertinent as the convection becomes deeper, is how the unsaturated environment is influenced by the enthalpy of vaporization made available through condensation in the cumulus drafts. Here the usual picture is one of cumulus clouds forcing isopycnal surfaces to adjust to some effective saturated adiabat in the saturated component of the flow. This can be thought of in terms of a redistribution of mass among isopycnal surfaces as shown in Figure 10. This leads to a tilt in the isopycnal surfaces that induces gravity waves, which in the absence of rotation act to flatten the isopycnals, thereby realigning them with the isobars (Bretherton & Smolarkiewicz 1989). From this point of view, the buoyancy (equivalently θ_v, which in the unsaturated environment is most dependent on temperature) adjusts on a timescale defined by the gravity wave speed in the cloud-free environment and the distance from the convection,

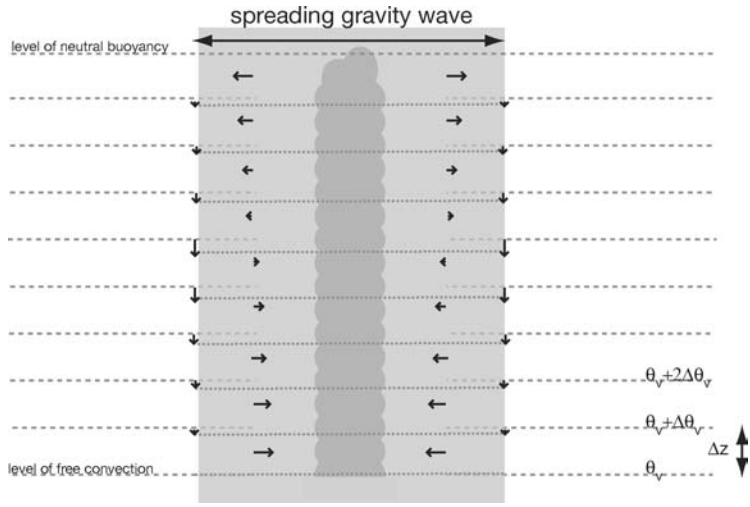

Figure 10 Schematic of adjustment owing to cumulus heating following Bretherton & Smolarkiewicz (1989). Here the transient adjustment to the moist-adiabatic lapse rate of the convecting tower from Figure 3 is shown to be accomplished by a spreading gravity wave front. As the subsidence wave moves away from the region of convection, it is associated with a downward displacement of isentropes, which equilibrates the buoyancy (θ_v) profile.

whereas the moisture field adjusts on a much slower timescale determined by the rate of horizontal stirring along isentropes and the rate at which the intercloud environment is subsiding. Because the gravity wave speed scales with the depth of the layer (reaching speeds of approximately 50 m/s for the gravest modes), this disparity between timescales is most evident for deep convection.

Deep precipitating cumuliform convection also differs from shallow cumuliform convection in terms of the range and significance of the larger-scale structures into which it so often aggregates. Generically, such features are called mesoscale convective systems, MCSs, which Houze (2004) defines as any "cumulonimbus cloud system that produces a contiguous precipitation area greater than 100 km in any one direction." This definition is sufficiently broad to include hurricanes as well as a wide variety of other agglomerations of convective clouds, and it recognizes what Mapes (1993) calls the gregarious nature of cumulus convection. Such systems typically share structural, rather than simply morphological, attributes. For instance, they are commonly associated with large regions of stratiform precipitation and organized mesoscale circulations, both of which interact with regions of more cellular cumulus convection thus warranting the nomenclature of system. The resultant circulation differs from a noninteracting envelope of cumulus clouds in many respects, ranging from its longevity, characteristics of propagation, and mechanisms for producing precipitation. A prototypical MCS is the squall line, which is illustrated by the schematic in Figure 11. This figure illustrates how

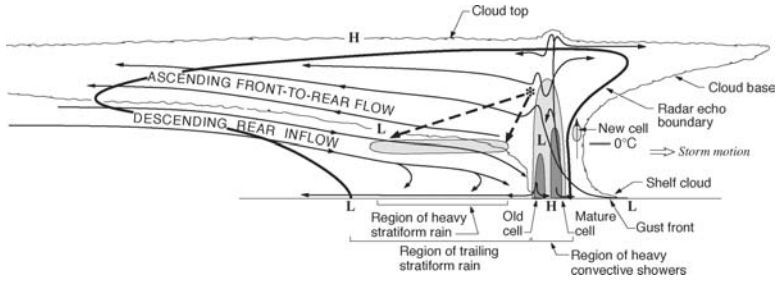

Figure 11 Example of a prototypical mesoscale convective system, a squall line. Taken from Houze (1989).

convective cells fuel a much larger circulation, which in turn helps organize and maintain and renew the convective cells. Here the circulation develops around deep, vigorous, convective cells arranged along a line going into the page. As they decay, they are swept back into the trailing stratiform graveyard, where through precipitation they help moisten and cool a low-level inflow of low θ_e air, which in turn helps form a pool of cold air near the surface whose leading-edge gust front helps initiate new convection. This couplet of upper-level front-to-rear flow and lower-level inflow is consistent with the response to deep convective heating shown in Figure 10 (Pandya & Durran 1996). Of the various forms of MCSs, the squall line is perhaps the best understood, with the idea being that the ambient wind shear is critical to the maintenance of such a structure (Rotunno et al. 1988). Indeed, almost all anisotropic forms of convective organization are thought to develop their anisotropy from the mean wind, although the details by which different structures are selected remains sketchy (Robe & Emanuel 2001). Even more uncertain is the extent to which systems self-aggregate independent of any organizing influence provided by the mean flow in which they are embedded.

5.2. Theoretical Perspectives

Many of the theoretical questions pertaining to precipitating cumuliform convection have counterparts in the discussion of the energetics of test parcels in Section 2.2 and the review of mass flux theories in Section 4. Arakawa (2004) casts this emphasis in terms of what he calls principal and supplementary closures: the former being some constraint on the intensity of convection (as measured by $M_{\rm cb}$ the cloud base mass flux), the latter being a constraint in form, typically in terms of a cloud model, which determines the vertical structure of the convection, i.e., $M(z)/M_{\rm cb}$. Unlike shallow convection, where $M_{\rm cb}$ is often determined by a budget constraint on the subcloud layer, or the velocity scale valid for the dry convective subcloud layer, for the case of precipitating cumuliform convection, the community has largely congealed around quasi-equilibrium ideas of Arakawa (1969), Arakawa & Schubert (1974), which constrain $M_{\rm cb}$ based on the temporally evolving energetics

of test parcels. In an early implementation of this idea Arakawa & Schubert (1974) argue that convection acts to just offset the destabilization of the atmosphere by nonconvective processes, where in this case the stability is measured with respect to the energetics of an ensemble of entraining plumes—in essence, their test parcels. This idea, and the cloud model underlying it, has been elaborated upon, simplified, and relaxed (e.g., Betts & Miller 1986, Emanual 1991, Moorthi & Suarez 1992, Zhang & McFarlane 1995, Raymond 1997, Pan & Randall 1998, Raymond et al. 2003), but in one form or another it serves as the conceptual foundation for almost all closures, largely displacing earlier ideas based solely on moisture constraints (see a discussion of these issues by Raymond & Emanual 1993). Nonetheless, the question of exactly how best to frame it, and how much the details matter, is a question of active research (Emanuel et al. 1994, Arakawa 2004).

A question of contemporary interest is the way in which the humidity of the free atmosphere may regulate convection. The basic idea is that convection into an especially dry atmosphere tends to be more readily diminished by entrainment of very dry air (Mapes & Zuidema 1996, Parsons et al. 2000). From this perspective, the spectrum of cloud depths in a convecting atmosphere, and hence precipitation, may be regulated not only by the thermal structure of the free-troposphere, but also its humidity structure, where the latter is modulated by intrusions of dry air into the convecting zones. Such effects are not evident in many theories of moist convection, and recent work has focused on better incorporating these and other effects, such as the regulating role of convective inhibition (Derbyshire et al. 2004, Mapes 2000). To the extent that these ideas of convection adjusting the atmosphere to some state of neutral stratification can be thought of as mean field theories, another exciting area of recent work concerns attempts to rationalize fluctuations (Buizza et al. 1999, Lin & Neelin 2000, Majda & Khouider 2002).

From the perspective of simulation, many interesting questions can and have been posed from the point of view of radiative convective equilibrium (e.g., Held et al. 1993, Robe & Emanuel 1996, Thompkins & Craig 1998). The geometry of this problem is one of an atmosphere that is being destabilized through a fixed depth H over a surface of fixed temperature. Convection then acts to equilibrate the atmosphere over this depth. The presence of many hidden scales, from moisture scale heights, precipitation, and ice formation timescales, etc., renders the basic configuration of the problem an open question; notwithstanding that the space and timescales encompassed by even the simplest configurations pose grand challenges for computation. For instance, to what extent should a realistic representation of radiative processes be included? What makes moist convection fascinating is its ability to be diabatic in so many different ways. In this vein, it is not clear that the diabatic tendency of precipitation formation is any more essential than the cloud's diabatic interaction with radiant streams of energy that drive the system in the first place (cf., Held et al. 1993). Although these types of calculations still challenge our computational capacity, they are beginning to be employed to ask fundamental questions. For instance, this framework has been used by Robe & Emanuel (2001) to investigate the interplay between the mean shear and convective organization, by

Thompkins (2001) to investigate the effect of water vapor feedbacks on convection, by Grabowski (2003) to investigate the interaction of convection with larger-scale circulations, and by Emanuel & Bister (1996), Pauluis & Held (2002a,b) to test theories of convective scaling. From the point of view of Pauluis & Held (2002a), deep convection can fruitfully be thought of as a reversible dehumidifier that in equilibrium is balanced by an irreversible rehumidification of dried air away from the convecting regions. The dehumidification/moistening cycle can be linked to the latent heat transport and limits the amount of energy available for the production of kinetic energy. This effect is sufficiently strong so that the dissipation in the shear zones in the wake of falling hydrometeors is larger than the dissipation of kinetic energy generated by convective accelerations (Pauluis et al. 2000), thus pointing to yet another way in which moist convection expresses its irreversibility.

6. SYNTHESIS

Throughout this review, I have attempted to emphasize how moist convection is many things, rather than one thing, an emphasis motivated by the question, What is moist convection? Such questions are often asked from the perspective of students of dry convection, for which the driving instability is easier to characterize, and for whom the corresponding question is consequently simpler to answer. One of the facets of moist convection that makes it such a vast, challenging, and difficult subject is the variety of regimes it encompasses, and the diversity of physical processes particular regimes embody, which is another way of saying that moist convection is many things, i.e., is driven by many underlying instabilities, most of which have no analog in dry convection. We should not, however, lose sight of the fact that beyond curiosity, much interest in moist convection is motivated by the need to accurately represent its effects in large-scale models for use in numerical weather prediction or in climate studies. This raises the question as to whether moist convection must be modeled in many ways, or if some simple set of ideas can provide a unified basis capable of representing its collective effects across a variety of regimes. For the better part of the past half century, work has adopted the former approach, with large-scale models often employing distinct, and increasingly complex, models to represent stratocumulus, versus trade-cumulus, versus deep cumulus convection. Some evidence of this is present in this review, where mass flux concepts dominate the discussion of cumuliform convection and mixed-layer theory (consistent with local mixing theories typified by eddy diffusion) dominates the discussion of moist convection in association with stratiform clouds. Bucking this trend is a renewed interest in simple models whose physical principles allow them to recognize a variety of forcings and naturally switch among regimes, from dry to stratocumulus convection, from shallow to deep convection, and from stratocumulus to trade-cumulus. For instance, Lappen & Randall (2001) and Golaz et al. (2002a) can in some sense be viewed as an attempt to blend mass-flux approaches with more standard turbulence closure theories used for dry

convection. Cheinet (2003) explores the unity of mass-flux concepts for dry convection, whereas Cheinet & Teixeira (2003) show that eddy-diffusivity approaches can express behavior usually reserved for mass flux models.

Motivated by a similar desire to represent moist convection with a single set of equations, increased computer power has made it possible to consider embedding two- or three-dimensional models whose discretization is chosen so as to represent convective drafts that span the troposphere but whose domains span some subset of the space of a large-scale grid volume in a three-dimensional model, as a basis for representing the collective effects of moist convection across regimes. This multiscale modeling framework has been referred to as cloud resolving convective parameterization (Grabowski & Smolarkiewicz 1999) and super-parameterization (Randall et al. 2003, Arakawa 2004). Although conceptually simple, such calculations are computationally intensive. Nonetheless, as they become increasingly common and begin to capture a wider range of scales within convecting atmospheres, they should prove useful in both bounding our expectations and (along with the ever increasing power of satellite remote sensing) enriching the phenomenology from which our insights and intuition are drawn, thus brightening the prospects for theoretical advancement.

7. SUMMARY

Unlike dry convection, moist convection is not one, but many things. I illustrate this by reviewing some essential aspects of moist convection, both in terms of its expression within the context of moist atmospheric thermodynamics and through a consideration of three paradigms: stratocumulus, shallow nonprecipitating, and deep precipitating convection. These problems highlight the many ways in which moist convection distinguishes itself, most fundamentally through its nonlocal interactions with other parts of the flow, either through radiative, gravity wave, or microphysical (precipitation) processes. For each regime, modern remote sensing is providing wondrous new insights, whether it be with respect to the statistics of precipitating convection and its interaction with the larger-scale environment as seen by satellite, or the structure of shallow cloud circulations and precipitation, as seen by surface-based or airborne cloud radars. Simulation, and appropriately simply simulation paradigms, are also being worked out for the various regimes. Together with long-standing techniques for probing the structure of moist convecting atmospheres, these approaches bode well for new leaps in understanding of one of nature's more majestic phenomena.

ACKNOWLEDGMENTS

Comments by and discussions with Akio Arakawa, Simona Bordoni, Stephan de Roode, Richard H. Johnson, Margaret A. LeMone, Brian Mapes, Olivier Pauluis, Joao Teixeira, Verica Savic Jovcic, Steven Sherwood, Pier Siebesma, Michio Yanai, and Edward J. Zipser helped clarify the exposition. Support for my time while

writing this review was provided by the National Science Foundation through Grant ATM-9985413.

The *Annual Review of Earth and Planetary Science* is online at http://earth.annualreviews.org

LITERATURE CITED

Albrecht BA. 1991. Fractional cloudiness and cloud-top entrainment instability. *J. Atmos. Sci.* 48:1519–25

Albrecht BA, Betts AK, Schubert WH, Cox SK. 1979. A model of the thermodynamic structure of the trade-wind boundary layer. Part I: Theoretical formulation and sensitivity tests. *J. Atmos. Sci.* 36:90–98

Arakawa A. 1969. Parameterization of cumulus clouds. In *Proc. WMO/IUGG Symp. Numer. Weather Predict.*, IV:106. Tokyo: World Meteorol. Organ.

Arakawa A. 1975. Modelling clouds and cloud processes for use in climate model. In *The Physical Basis of Climate and Climate Modelling, GARP Publ. Ser.* 16:183–74. Tokyo: World Meteorol. Organ.

Arakawa A. 2004. The cumulus parameterization problem: past, present, and future. *J. Clim.* 17:2493–525

Arakawa A, Schubert WS. 1974. Interaction of a cumulus cloud ensemble with the large-scale environment. Part I. *J. Atmos. Sci.* 31: 674–701

Asai T, Kasahara A. 1967. A theoretical study of the compensating downward motions associated with cumulus clouds. *J. Atmos. Sci.* 24:487–96

Austin P, Wang Y, Pincus R, Kujala V. 1995. Precipitation in stratocumulus clouds: Observational and modeling results. *J. Atmos. Sci.* 52:2329–52

Bechtold P, Siebesma P. 1998. Organization and representation of boundary layer clouds. *J. Atmos. Sci.* 55(5):888–95

Bellon G, Stevens B. 2005. On bulk models of shallow cumulus convection. *J. Atmos. Sci.* In press

Benner T, Curry JA. 1998. Characteristics of small tropical cumulus clouds and their impact on the environment. *J. Geophys. Res.* 103(28):28753–67

Betts AK. 1973. Non-precipitating cumulus convection and its parameterization. *Q. J. R. Meteorol. Soc.* 99:178–96

Betts AK. 1997. *The Physics and Parameterization of Moist Atmospheric Convection*. Chapter 4: *Trade Cumulus: Observations and Modelling*, pp. 99–126. Dordrecht, The Neth.: Kluwer

Betts AK, Albrecht B. 1987. Conserved variable analysis of the convective boundary layer thermodynamic structure over the tropical ocean. *J. Atmos. Sci.* 44:83–99

Betts AK, Miller MJ. 1986. A new convective adjustment scheme. Part II: Single column tests using GATE wave, BOMEX ATEX and arctic airmass data sets. *Q. J. R. Meteorol. Soc.* 112:693–709

Betts AK, Ridgway W. 1989. Climatic equilibrium of the atmospheric convective boundary layer over a tropical ocean. *J. Atmos. Sci.* 46:2621–41

Bjerknes J. 1938. Saturated-adiabatic ascent of air through dry-adiabatically descending environment. *Q. J. R. Meteorol. Soc.* 64:325–30

Blyth AM. 1993. Entrainment in cumulus clouds. *J. Appl. Meteorol.* 32:626–41

Bohren CF, Albrecht BA. 1998. *Atmospheric Thermodynamics*. New York: Oxford Univ. Press

Bougeault P. 1985. The diurnal cycle of the marine stratocumulus layer: A higher-order model study. *J. Atmos. Sci.* 42:2826–43

Bretherton CS. 1993. Understanding Albrecht's model of trade cumulus cloud fields. *J. Atmos. Sci.* 50:2264–83

Bretherton CS, Austin P, Siems ST. 1995. Cloudiness and marine boundary layer dynamics in the ASTEX lagrangian experiments. Part II: Cloudiness, drizzle, surface fluxes, and entrainment. *J. Atmos. Sci.* 52:2724–35

Bretherton CS, Peters ME, Back LE. 2004b. Relationships between water vapor path and precipitation over the tropical oceans. *J. Clim.* 17:1517–28

Bretherton CS, Smolarkiewicz PK. 1989. Gravity waves, compensating subsidence and detrainment around cumulus clouds. *J. Atmos. Sci.* 46:740–59

Bretherton CS, Uttal T, Fairall CW, Yuter S, Weller R, et al. 2004a. The EPIC 2001 stratocumulus study. *Bull. Am. Meteorol. Soc.* 85:967–77

Bretherton CS, Wyant MC. 1997. Moisture transport, lower tropospheric stability, and decoupling of cloud-topped boundary layers. *J. Atmos. Sci.* 54:148–67

Brown AR, Grant AM. 2000. Extensions to a similiarty hypothesis for shallow cumulus convection. *Bound.-Layer Meteorol.* 97:173–90

Buizza R, Miller M, Palmer TN. 1999. Stochastic representation of model uncertainties in the ECMWF Ensemble Prediction System. *Q. J. R. Meteorol. Soc.* 125:2887–908

Cheinet S. 2003. A multiple mass flux parameterization for the surface-generated convection. Part I: Dry plumes. *J. Atmos. Sci.* 60:2313–27

Cheinet S. 2004. A multiple mass flux parameterization for the surface-generated convection. Part II: Cloudy cores. *J. Atmos. Sci.* 61:1093–113

Cheinet S, Teixeira J. 2003. A simple formulation for the eddy-diffusivity parameterization of cloud-topped boundary layers. *Geophys. Res. Lett.* 30:1930

Ciesielski PE, Schubert WH, Johnson RH. 2001. Diurnal variability of the marine boundary layer during ASTEX. *J. Atmos. Sci.* 58:2355–76

Comstock KK, Wood R, Yuter SE, Bretherton CS. 2004. Reflectivity and rain rate in and below drizzling stratocumulus. *Q. J. R. Meteorol. Soc.* 130:2891–918

Cotton WR, Anthes RA. 1989. *Storm and Cloud Dynamics*. San Diego: Academic Press. 880 pp.

Deardorff JW. 1970. Convective velocity and temperature scales for the unstable planetary boundary layer and for Rayleigh convection. *J. Atmos. Sci.* 27:1211–13

Deardorff JW. 1980. Cloud top entrainment instability. *J. Atmos. Sci.* 37:131–47

Derbyshire S, Beau I, Bechtold P, Grandpeix J, Piriou J, et al. 2004. Sensitivity of moist convection to environmental humidity. *Q. J. R. Meteorol. Soc.* 130:3055–80

De Roode SR, Duynkerke PG. 1997. Observed Lagrangian transition of stratocumulus into cumulus during ASTEX: mean state and turbulence structure. *J. Atmos. Sci.* 54:2157–73

Duynkerke PG. 1989. Diurnal variation of a marine stratocumulus layer: a model sensitivity study. *Mon. Weather Rev.* 117:1710–25

Duynkerke PG. 1993. The stability of cloud top with regard to entrainment: amendment of the theory of cloud-top entrainment instability. *J. Atmos. Sci.* 50:495–502

Emanuel KA. 1991. A scheme for representing cumulus convection in large-scale models. *J. Atmos. Sci.* 48:2313–35

Emanuel KA. 1994. *Atmospheric Convection*. New York: Oxford Univ. Press. 580 pp.

Emanuel KA, Bister M. 1996. Moist convective velocity and buoyancy scales. *J. Atmos. Sci.* 53:3276–85

Emanuel KA, Neelin DJ, Bretherton CS. 1994. On large-scale circulations in convecting atmospheres. *Q. J. R. Meteorol. Soc.* 120:1111–43

Feingold G, Morley B. 2003. Aerosol hygroscopic properties as measured by lidar and comparison with in situ measurements. *J. Geophys. Res.* 108:D11. doi:10.1029/2002JD002842

Golaz J, Larson VE, Cotton WR. 2002a. A PDF based model for boundary layer clouds. Part I: method and model description. *J. Atmos. Sci.* 59(24):3540–51

Golaz J, Larson VE, Cotton WR. 2002b. A PDF

based model for boundary layer clouds. Part II: model results. *J. Atmos. Sci.* 59(24):3552–71

Grabowski WW. 2003. MJO-like coherent structures: sensitivity simulations using cloud-resolving convection parameterization CRCP. *J. Atmos. Sci.* 60:847–64

Grabowski WW, Smolarkiewicz PK. 1999. CRCP: a cloud resolving convection parameterization for modeling the tropical convective atmosphere. *Physica D* 133:171–78

Grant ALM. 2001. Cloud base fluxes in the cumulus-capped boundary layer. *Q. J. R. Meteorol. Soc.* 127(572):407–21

Grant ALM, Brown AR. 1999. A similarity hypothesis for shallow cumulus transports. *Q. J. R. Meteorol. Soc.* 125(558):1913–36

Held IM, Hemler RS, Ramaswamy V. 1993. Radiative-convective equilibrium with explicit two-dimensional moist convection. *J. Atmos. Sci.* 50:767–82

Houze RA. 1989. Observed structure of mesoscale convective systems and implications for large-scale heating. *Q. J. R. Meteorol. Soc.* 115:425–46

Houze RA. 1993. *Cloud Dynamics*. San Diego: Academic. 573 pp.

Houze RA. 1997. Stratiform precipitation in regions of convection: a meteorological paradox? *Bull. Am. Meteorol. Soc.* 78:2179–96

Houze RA. 2004. Mesoscale convective systems. *Rev. Geophys.* 42:RG4003, doi:10.1029/2004RG000150

Iribarne JV, Godson WL. 1973. *Atmospheric Thermodynamics*. Dordrecht, Holl.: D Reidel

Jensen JB, Lee S, Krummel PB, Katzfey J, Gogoasa D. 2000. Precipitation in marine cumulus and stratocumulus. Part I: Thermodynamic and dynamic observations of closed cell circulations and cumulus bands. *Atmos. Res.* 54:117–55

Johnson RH. 1976. The role of convective-scale precipitation downdrafts in cumulus and synoptic-scale interactions. *J. Atmos. Sci.* 33:1890–910

Johnson RH, Lin X. 1997. Episodic trade wind regimes over the western pacific warm pool. *J. Atmos. Sci.* 54:2020–34

Johnson RH, Rickenbach TM, Rutledge SA, Ciesielski PE, Schubert WH. 1999. Trimodal characteristics of tropical convection. *J. Clim.* 12:2397–418

Klein SA. 1997. Synoptic variability of low-cloud properties and meteorological parameters in the subtropical trade wind boundary layer. *J. Clim.* 10:2018–39

Klein SA, Hartmann DL. 1993. The seasonal cycle of low stratiform clouds. *J. Clim.* 6:1587–606

Kollias P, Albrecht BA, Lhermitte R, Savtchenko A. 2001. Radar observations of updrafts, downdrafts and turbulence in fair-weather cumuli. *J. Atmos. Sci.* 58:1750–66

Kraus EB. 1963. The diurnal precipitation change over the sea. *J. Atmos. Sci.* 20:551–56

Kraus H, Schaller E. 1978. A note on the closure in Lilly-type inversion models. *Tellus* 30:284–488

Krueger SK, McLean GT, Fu Q. 1995. Numerical simulation of stratus-to-cumulus transition in the subtropical marine boundary layer. Part I: Boundary layer structure. *J. Atmos. Sci.* 52:2839–50

Kuo H-C, Schubert W. 1988. Stability of cloud-topped boundary layers. *Q. J. R. Meteorol. Soc.* 114:887–916

Lappen C-L, Randall DA. 2001. Toward a unified parameterization of the boundary layer and moist convection. Part I: A new type of mass-flux model. *J. Atmos. Sci.* 58:2021–36

LeMone MA, Pennell WT. 1976. The relationship of trade wind cumulus distribution to sublcoud layer fluxes and structure. *Mon. Weather Rev.* 104:524–39

LeMone MA, Zipser EJ. 1980. Cumulonimbus vertical velocity events in GATE. Part I: Diameter, intensity and mass flux. *J. Atmos. Sci.* 37:2444–57

Lewellen DC, Lewellen W. 1998. Large-eddy boundary layer entrainment. *J. Atmos. Sci.* 55:2645–65

Lewellen DC, Lewellen W. 2002. Entrainment and decoupling relations for cloudy boundary layers. *J. Atmos. Sci.* 59:2966–86

Lilly DK. 1968. Models of cloud topped mixed layers under a strong inversion. *Q. J. R. Meteorol. Soc.* 94:292–309

Lilly DK. 2002. Entrainment into cloud-topped mixed layers: A new closure. *J. Atmos. Sci.* 59:3353–61

Lin JW-B, Neelin JD. 2000. Influence of stochastic convection on tropical intraseasonal variability. *Geophy. Res. Lett.* 27:3691–94

Lock AP. 1998. The parameterization of entrainment in cloudy boundary layers. *Q. J. R. Meteorol. Soc.* 124:2729–53

López RE. 1977. The lognormal distribution and cumulus cloud populations. *Mon. Weather Rev.* 105:865–72

MacVean MK, Mason PJ. 1990. Cloud-top entrainment instability through small-scale mixing and its parameterization in numerical models. *J. Atmos. Sci.* 47:1012–30

Majda AJ, Khouider B. 2002. Stochastic and mesoscopic models for tropical convection. *Proc. Natl. Acad. Sci. USA* 99:1123–28

Malkus JS. 1954. Some results of a trade-cumulus cloud investigation. *J. Meteorol.* 11:220–37

Malkus JS. 1956. On the maintenance of the trade winds. *Tellus* 8:335–50

Malkus JS. 1958. On the structure of the trade wind moist layer. *Pap. Phys. Oceanogr. Meteorol.* 13(2):1–47

Manins PC, Turner JS. 1978. Relation between the flux ratio and energy ratio in convectively mixed layers. *Q. J. R. Meteorol. Soc.* 104:39–44

Mapes BE. 1993. Gregarious tropical convection. *J. Atmos. Sci.* 50:2026–37

Mapes BE. 2000. Convective inhibition, subgrid-scale triggering energy, and stratiform instability in a toy tropical wave model. *J. Atmos. Sci.* 57:1515–35

Mapes BE, Zuidema P. 1996. Radiative-dynamical consequences of dry toungues in the tropical troposphere. *J. Atmos. Sci.* 53:620–38

McCaa JR, Bretherton C. 2004. A new parameterization for shallow cumulus convection and its application to marine subtropical cloud-topped boundary layers. Part II: Regional simulations of marine boundary layer clouds. *Mon. Weather Rev.* 132:883–96

Moeng C-H. 1998. Stratocumulus-topped atmospheric planetary boundary layer. In *Buoyant Convection in Geophysical Flows*, ed. EJ Plate, EE Fedorovich, DX Viegas, JC Wyngaard, 513:421–40. Dordrecht, The Neth.: Kluwer Acad.

Moeng C-H. 2000. Entrainment rate, cloud fraction and liquid water path of PBL stratocumulus clouds. *J. Atmos. Sci.* 57:3627–43

Moeng C-H, Stevens B. 1999. Marine stratocumulus and its representation in GCMs. In *General Circulation Model Development: Past, Present, and Future*, ed. DA Randall, pp. 577–604. New York: Elsevier

Moeng C-H, Sullivan PP, Stevens B. 1999. Including radiative effects in an entrainment-rate formula for buoyancy driven PBLs. *J. Atmos. Sci.* 56:1031–49

Moncrieff M. 1997. Momentum transport by organized convection. See Smith 1997, pp. 231–53

Moorthi S, Suarez MJ. 1992. Relaxed Arakawa-Schubert: a parameterization of moist convection for general circulation models. *Mon. Weather Rev.* 120:978–1002

Nakazawa T. 1988. Tropical super clusters within intraseasonal variations over the western Pacific. *J. Meteorol. Soc. Jpn.* 66:823–39

Neggers RA, Jonker HJJ, Siebesma AP. 2003. Size statistics of cumulus cloud populations in large-eddy simulations. *J. Atmos. Sci.* 60:1060–74

Neggers RA, Siebesma AP, Jonker HJJ. 2002. A multiparcel model for shallow cumulus convection. *J. Atmos. Sci.* 59:1655–67

Neiburger M, Johnson DS, Chien C-W. 1961. *Studies of the structure of the atmosphere over the eastern Pacific ocean in summer*. Tech. Rep., Univ. Calif., Berkeley. 94 pp.

Nesbitt SW, Zipser EJ. 2003. The diurnal cycle of rainfall and convective intensity according to three years of TRMM measurements. *J. Clim.* 16:1456–75

Nesbitt SW, Zipser EJ, Cecil DJ. 2000. A census of precipitation features in the tropics using

TRMM: Radar, ice scattering and ice observations. *J. Clim.* 13:4087–106

Nicholls S. 1984. The dynamics of stratocumulus: Aircraft observations and comparisons with a mixed layer model. *Q. J. R. Meteorol. Soc.* 110:783–820

Nicholls S, LeMone MA. 1980. The fair weather boundary layer in GATE: the relationship of subcloud fluxes and structure to the distribution and enhancement of cumulus cloud. *J. Atmos. Sci.* 37:2051–67

Nitta T, Esbensen S. 1974. Heat and moisture budget analyses using BOMEX data. *Mon. Weather Rev.* 102:17–28

Ötles Z, Young JA. 1996. Influence of shallow cumuli on subcloud turbulence fluxes analzyed from aircraft data. *J. Atmos. Sci.* 53:665–76

Paluch IR, Lenschow DH. 1991. Stratiform cloud formation in the marine boundary layer. *J. Atmos. Sci.* 48:2141–57

Pan D-M, Randall DA. 1998. A cumulus parameterization with a prognostic closure. *Q. J. R. Meteorol. Soc.* 124:949–81

Pandya RE, Durran DR. 1996. The influence of convectively generated thermal forcing on the mesoscale circulation around squall lines. *J. Atmos. Sci.* 53:2924–51

Parsons DB, Yoneyama K, Redelsperger J-L. 2000. The evolution of the tropical western Pacific atmosphere-ocean system following the arrival of a dry intrusion. *Q. J. R. Meteorol. Soc.* 126(563):517–48

Pauluis O, Balaji V, Held IM. 2000. Frictional dissipation in a precipating atmosphere. *J. Atmos. Sci.* 57:989–94

Pauluis O, Held IM. 2002a. Entropy budget of an atmosphere in radiative-convective equilibrium. Part I: Maximum work and frictional dissipation. *J. Atmos. Sci.* 59:125–39

Pauluis O, Held IM. 2002b. Entropy budget of an atmosphere in radiative-convective equilibrium. Part II: Latent heat transport and moist processes. *J. Atmos. Sci.* 59:140–49

Pincus R, Baker MB, Bretherton CS. 1997. What controls stratocumulus radiative properties? Lagrangian observations of cloud evolution. *J. Atmos. Sci.* 54:2215–36

Plank VG. 1969. The size distribution of cumulus clouds in representative Florida populations. *J. Appl. Meteorol.* 8:46–67

Randall D, Khairoutdinov M, Arakawa A, Grabowski W. 2003. Breaking the cloud parameterization deadlock. *Bull. Am. Meteorol. Soc.* 84(11):1547–64

Randall DA. 1980. Conditional instability of the first kind upside-down. *J. Atmos. Sci.* 37:125–30

Randall DA, Schubert WH. 2004. *Atmospheric Turbulence and Mesoscale Meteorology*. Chapter 4: *Dreams of a Stratocumulus Sleeper*, pp. 71–96. Cambridge, NY: Cambridge Univ. Press

Randall DA, Wang J. 1992. The moist available energy of a conditionally unstable atmosphere. *J. Atmos. Sci.* 49:240–55

Raymond DJ. 1997. Boundary layer quasi-equilibrium (BLQ). See Smith 1997, pp. 387–96

Raymond DJ, Blyth AM. 1986. A stochastic model for non-precipitating convection. *J. Atmos. Sci.* 43:2708–18

Raymond DJ, Emanuel KA. 1993. The Kuo cumulus parameterization. In *The Representation of Cumulus Convection in Numerical Models*, ed. KA Emanuel, DJ Raymond, *Meteor. Monogr.*, 24(No. 46):145–50. Boston: Am. Meteorol.

Raymond DJ, Raga GB, Bretherton CS, Molinari J, Lopez-Carrillo C, Fuchs Z. 2003. Convective forcing in the intertropical convergence zone of the eastern Pacific. *J. Atmos. Sci.* 6017:2064–82

Redelsperger J-L. 1997. The mesoscale organization of deep convection. See Smith 1997, pp. 59–98

Reed RJ, Recker EE. 1971. Structure and properties of synoptic-scale wave disturbances in the equatorial western Pacific. *J. Atmos. Sci.* 28:1117–33

Riehl H, Yeh C, Malkus JS, LaSeur NE. 1951. The North-East Trade of the Pacific Ocean. *Q. J. R. Meteorol. Soc.* 77:598–626

Robe FR, Emanuel KA. 1996. Moist convective scaling: some inferences from

three-dimensional cloud ensemble simulations. *J. Atmos. Sci.* 53:3265–75

Robe FR, Emanuel KA. 2001. The effect of vertical wind shear on radiative-convective equilibrium states. *J. Atmos. Sci.* 58:1427–45

Rotunno R, Klemp JB, Weisman ML. 1988. A theory for long-lived squall lines. *J. Atmos. Sci.* 45:463–85

Schubert WH. 1976. Experiments with Lilly's cloud-topped mixed layer model. *J. Atmos. Sci.* 33:436–46

Schubert WH, Wakefield JS, Steiner EJ, Cox SK. 1979. Marine stratocumulus convection. Part I: Governing equations and horizontally homogeneous solutions. *J. Atmos. Sci.* 36:1286–307

Schumacher C, Houze RA. 2003. Stratiform rain in the tropics as seen by the TRMM precipitation radar. *J. Clim.* 16:1739–56

Sherwood SC. 2000. On moist stability. *Mon. Weather Rev.* 128:4139–42

Sherwood SC, Dessler AE. 2001. A model for transport across the tropical tropopause. *J. Atmos. Sci.* 58:765–79

Short DA, Nakamura K. 2000. TRMM radar observations of shallow precipitation over the tropical oceans. *J. Clim.* 13(23):4107–24

Siebesma AP. 1998. Shallow convection. In *Buoyant Convection in Geophysical Flows*, ed. EJ Plate, EE Fedorovich, DX Viegas, JC Wyngaard, 513:441–86. Dordrecht, The Neth.: Kluwer Acad. 491 pp.

Siebesma AP, Brown CSBA, Chlond A, Cuxart J, Duynkerke P, et al. 2003. A large-eddy simulation study of shallow cumulus convection. *J. Atmos. Sci.* 60:1201–19

Siebesma AP, Cuijpers JWM. 1995. Evaluation of parametric assumptions for shallow cumulus convection. *J. Atmos. Sci.* 52:650–66

Siebesma AP, Jonker HJJ. 2000. Anomalous scaling of cumulus cloud boundaries. *Phys. Rev. Lett.* 85(1):214–17

Siems ST, Bretherton CS. 1992. A numerical investigation of cloud-top entrainment instability and related experiments. *Q. J. R. Meteorol. Soc.* 118:787–818

Simpson J, Wiggert V. 1969. Models of precipitating cumulus towers. *Mon. Weather Rev.* 97:471–89

Smith RK, ed. 1997. *The Physics and Parameterization of Moist Atmospheric Convection*. NATO ASI. Dordrecht, The Neth.: Academic. 498 pp.

Stage SA, Businger JA. 1981. A model for entrainment into a cloud-topped marine boundary layer. Part I: Model description and application to a cold-air outbreak epsiode. *J. Atmos. Sci.* 38:2213–29

Stevens B. 2000. Cloud transitions and decoupling in shear-free stratocumulus-topped boundary layers. *Geophy. Res. Lett.* 27:2557–60

Stevens B. 2002. Entrainment in stratocumulus mixed layers. *Q. J. R. Meteorol. Soc.* 128:2663–90

Stevens B. 2004. Similarity relations for shallow cumulus convection. In *16th Symp. Boundary Layers Turbulence, Portland, ME*. Boston: Am. Meteorol. Soc.

Stevens B, Ackerman AA, Albrecht BA, Brown AR, Chlond A, et al. 2001. Simulations of trade-wind cumuli under a strong inversion. *J. Atmos. Sci.* 58:1870–91

Stevens B, Lenschow DH, Faloona I, Moeng C-H, Lilly DK, et al. 2003. On entrainment in nocturnal marine stratocumulus. *Q. J. R. Meteor. Soc.* 129:3469–92

Stevens B, Vali G, Comstock K, Wood R, van Zanten MC, et al. 2005. Pockets of open cells and drizzle in marine stratocumulus. *Bull. Am. Meteorol. Soc.* 86:51–57

Tompkins AM. 2001. Organization of tropical convection in low vertical wind shears: the role of water vapor. *J. Atmos. Sci.* 58:529–45

Tompkins AM, Craig GC. 1998. Radiative-convective equilibrium in a three-dimensional cloud-ensemble model. *Q. J. R. Meteorol. Soc.* 124:2073–97

Tiedtke M. 1989. A comprehensive mass flux scheme for cumulus parameterization in large-scale models. *Mon. Weather Rev.* 117: 1779–800

Tiedtke M, Heckley WA, Slingo J. 1988. Tropical forecasting at ECMWF: the influence of physical parametrization on the mean

structure of forecasts and analyses. *Q. J. R. Meteorol. Soc.* 114:639–64

Tung W-W, Lin C, Chen B, Yanai M, Arakawa A. 1999. Basic modes of cumulus heating and drying observed during TOGA-COARE IOP. *Geophy. Res. Lett.* 26:3117–20

Turton JD, Nicholls S. 1987. A study of the diurnal variation of stratocumulus using a multiple mixed layer model. *Q. J. R. Meteorol. Soc.* 113:969–1009

van Zanten MC, Duynkerke PG, Cuijpers JWM. 1999. Entrainment parameterization in convective boundary layers derived from large eddy simulations. *J. Atmos. Sci.* 56:813–28

van Zanten MC, Stevens B, Vali G, Lenschow DH. 2004. On drizzle rates in nocturnal marine stratocumulus. *J. Atmos. Sci.* 62:88–106

Verkley WTM, Gerkema T. 2004. On maximum entropy profiles. *J. Atmos. Sci.* 61:931–36

Vernon EM. 1936. The diurnal variation in ceiling height beneath stratus clouds. *Mon. Weather Rev.* 64:14–16

von Ficker H. 1936. Die Passatinversion. *Veröffentlichungen Meteorol., Inst. Univ. Berlin*, pp. 1–33

Wang S. 1993. Modeling marine boundary-layer clouds with a two-layer model: A one dimensional simulation. *J. Atmos. Sci.* 50:4001–21

Wang S, Wang Q. 1994. Roles of drizzle in a one-dimensional third-order turbulence closure model of the nocturnal stratus-topped marine boundary layer. *J. Atmos. Sci.* 51:1559–76

Yanai M, Esbensen S, Chu J-H. 1973. Determination of bulk properties of tropical cloud clusters from large-scale heat and moisture budgets. *J. Atmos. Sci.* 30:611–27

Yin B, Albrecht B. 2000. Spatial variability of atmospheric boundary layer structure over the eastern equatorial Pacific. *J. Clim.* 13:1574–92

Zhang GJ, McFarlane NA. 1995. Sensitivity of climate simulations to the parameterization of cumulus convection in the Canadian Climate Centre General Circulation Model. *Atmos.-Ocean* 33:407–46

Zipser E. 1969. The role of organized unsaturated convective downdrafts in the structure and rapid decay of an equatorial disturbance. *J. Appl. Meteorol.* 8:799–814

Zipser EJ. 2003a. Some views on "hot towers" after 50 years of tropical field programs and two years of TRMM data. In *Cloud Systems, Hurricanes, and the Tropical Rainfall Measuring Mission (TRMM): A Tribute to Dr. Joanne Simpson.* Meteorol. Monogr., 29(No. 51):37–47. Boston: Am. Meteorol. Soc.

Zipser EJ. 2003b. Tropical precipitating systems. In *Handbook of Weather, Climate and Water: Dynamics, Climate, Physical Meteorology, Weather Systems and Measurements*, ed. TD Potter, BR Colman, pp. 62139. New York: Wiley. 1000 pp.

Zipser EJ, LeMone MA. 1980. Cumulonimbus vertical velocity events in GATE. Part II: Synthesis and model core structure. *J. Atmos. Sci.* 37:2458–69

Annual Review of Earth and Planetary Sciences
Volume 33, 2005

CONTENTS